Materials & Design 217 (2022) 110605

Contents lists available at ScienceDirect

Materials & Design

journal homepage: www.elsevier.com/locate/matdes

Atomic-scale understanding of oxidation mechanisms of materials by computational approaches: A review

Xingfan Zhang [a,b,1], Peiru Zheng [a,1], Yingjie Ma [a], Yanyan Jiang [a,*], Hui Li [a,*]

[a] Key Laboratory for Liquid–Solid Structural Evolution and Processing of Materials, Ministry of Education, Shandong University, Jinan 250061, China
[b] Kathleen Lonsdale Materials Chemistry, Department of Chemistry, University College London, 20 Gordon Street, London WC1H 0AJ, UK

HIGHLIGHTS

- Various computational techniques are widely used in modelling the atomic-scale oxidation of materials.
- Defects play a central role in determining oxidation kinetics and oxide growth patterns.
- Low-dimensional materials could have distinct oxidation mechanisms compared with their bulk counterparts, resulting in novel nanostructures.
- Current challenges and future prospects of computational modelling of surface reactions is discussed.

GRAPHICAL ABSTRACT

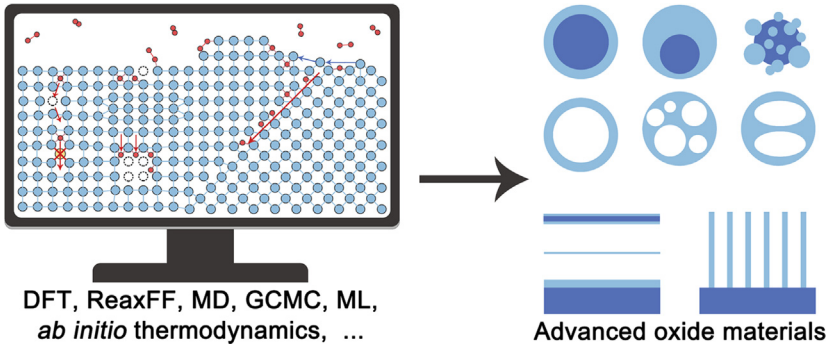

ARTICLE INFO

Article history:
Received 1 December 2021
Revised 14 March 2022
Accepted 28 March 2022
Available online 29 March 2022

ABSTRACT

The urgent requirement of minimising the worldwide cost of corrosion, accompanied by the increasingly pivotal role of advanced oxide materials, highlights the importance of understanding the mechanisms of material oxidation at the atomic level, which could help us to precisely control the oxidation processes. Nowadays, we are able to model and predict how the surface structures of materials evolve during oxidation based on the cross-fertilisation of various computational techniques. This review first overviews the state-of-the-art first-principles and force-field-based approaches for modelling surface reactions. Then, classical theories and recent advances in understanding the atomic-scale oxidation of bulk materials are introduced, from the initial solid-gas interactions to the subsequent oxide film growth. Defect-promoted oxidation mechanisms will be discussed in detail. Finally, distinct oxidation mechanisms of nanomaterials are discussed, including nanoparticles, nanowires, and two-dimensional materials, which are significantly different from their bulk counterparts and could result in novel oxide nanostructures with unique properties. This review provides a systematic overview of the central role of computational techniques in probing the atomic-scale oxidation mechanisms, which could further guide the synthesis of oxide-based cutting-edge materials such as ultra-thin oxide films and hollow oxide nanostructures.

Abbreviations: 2D, two-dimensional; AIMD, *ab initio* molecular dynamics; ANP, aluminium nanoparticle; COMB, charge-optimized many-body; CTIP, charge transfer ionic potential; DFT, density functional theory; ECW, embedded correlated wave function; ETEM, environmental transmission electron microscopy; FEM, finite element modelling; fs, femtosecond; GB 4-8, grain boundaries with 4-8 carbon rings; GB 5-8-5A1, grain boundaries with 5-8-5 carbon rings; GB 5-8-5D, grain boundaries with 5-8-5 carbon ringss; GCBH, grand canonical basin hopping; GCMC, grand canonical Monte Carlo; HPC, high-performance computing; MD, molecular dynamics; ML, machine learning; MVD, multi-vacancy defect; NEB, nudged elastic band; PG, pristine grapheme; QM, quantum mechanics; ReaxFF, reactive force-field; ReaxFF-MD or RMD, ReaxFF molecular dynamics; SVD, single-vacancy defect; μs, microsecond.

* Corresponding authors.
E-mail addresses: yanyan.jiang@sdu.edu.cn (Y. Jiang), lihuilmy@hotmail.com (H. Li).
[1] These authors contributed equally to this work: Xingfan Zhang and Peiru Zheng.

https://doi.org/10.1016/j.matdes.2022.110605
0264-1275/

Contents

1. Introduction

As one of the most important physicochemical processes in nature, oxidation occurs as discrete, atomistic events that involve the molecular adsorption on solids, forming and breaking of chemical bonds, atomic diffusion, and reconstruction of surface structures. In the precomputation era, it was nearly impossible to explore these atomic-level reactive events on material surfaces without modern *in situ* characterisation techniques. Physical models and theories on solid–gas interactions were also greatly restricted by the lack of accurate experimental data. However, with great effort and imagination, many outstanding experimentalists and theorists explored the mechanism and real-time process of oxidation and met with awe-inspiring achievement. Cabrera and Mott [1] proposed a reasonable explanation for the metal oxidation in 1949, which solved the problems of the kinetics and driving force of the low-temperature oxide film growth on metal surfaces as observed in many experiments. Their theory has been widely accepted and extended to a wide range of systems such as nanoparticles, nanowires, and liquid metals, which significantly inspired the continuous studies of oxidation mechanisms and oxidation-based material synthesis methods [2–9].

Oxidation is traditionally regarded as a costly and detrimental event usually linked with corrosion and materials degradation, which could result in severe consequences such as economic loss, environmental pollution, and casualty accidents [10,11]. Anti-oxidation and corrosion protection have become critical concerns in not only metallic materials but also novel technological fields such as perovskite solar cells [12] and catalysis [13,14]. On the other hand, oxidation can be valuable under controlled circumstances, which is one of the crucial techniques for fabricating cutting-edge oxide-based materials. For example, ultrathin oxide films have aroused considerable interest in electronics and spintronics [15], in which photon-assisted oxidation is a promising technique to control the oxygen non-stoichiometry [16]. Recently, liquid metals are also identified as ideal platforms for direct synthesis of two-dimensional (2D) oxides, in which Cabrera-Mott theory remains valid [8,17,18]. Hollow and nanoporous metal oxide nanostructures can be synthesised through the oxidation-induced Kirkendall cavitation process, which can be used in energy harvesting and conversion applications [19–22]. Oxide nanowires can also be grown on metal substrates during controlled oxidation [23].

Despite the great advances that had been made, the detailed understanding of material oxidation at the atomic level was still lacking. In particular, how oxygen interacts with materials and affects their properties remained elusive, which is the key to developing next-generation anti-corrosion materials with enhanced protective performance and advanced electronic devices with excellent chemical stability [24–27]. For instance, oxygen has been found to damage the chemical stability of hybrid organic–inorganic perovskites but enhance the charge carrier lifetime [26,28,29]. Recently, non-oxidised bare Cu nanoparticles have been achieved with the assistance of surface-accumulated excess electrons that suppress oxygen adsorption, which initiated a new phase for replacing noble metals in catalytic applications [30]. However, the existing experimental approaches play a limited role in revealing the atomic-scale oxidation mechanisms. In recent years, various state-of-the-art computational approaches have been developed and improved in response to the proper time and conditions.

In the past few decades, with the rapid development of computer hardware, quantum mechanics (QM), and modern algorithms, computer modelling provides the capacity to model, probe, and analyse physicochemical reactions, making it possible to visualise the atomic-level reaction processes in real-time and predict the accurate energetics during the reactions. Computational approaches rapidly extended to all areas of chemistry and have been helping us answer unresolved questions about physicochemical phenomena and develop new theories. Without costly experiment conditions, computational approaches enable us to design advanced molecules and novel materials for various applications in a high-throughput way. A variety kinds of modelling methods have emerged and been widely employed, such as QM calculations, density functional theory (DFT) calculations [31,32], molecular dynamics (MD) simulations [33], Monte Carlo (MC) simulations [34], *ab initio* molecular dynamics (AIMD) [35], *ab initio* thermodynamics [36], QM/MM calculations [37], each elucidating its own advantages and speciality. Unlike typical chemical reactions, modelling the oxidation of materials requires relatively large model systems and should cover rather a long timescale to understand the dynamic oxide growth process. At present, there is no single modelling technique that can cover all the time and length scales within reasonable computational cost and at a high level of accuracy, and one must make use of multiscale methods in practical circumstances.

In this review, we start by introducing a series of computational techniques that are relevant to modelling the oxidation of materials, including their fundamental concepts and applications. Then, the fundamental oxidation mechanisms of bulk materials will be reviewed from the classical Cabrera-Mott theory to recent advances. The initial stage of surface oxidation, i.e., from the solid-oxygen interaction to the surface reconstruction, will be systematically introduced at the atomic level. Finally, the oxidation mechanisms of nanomaterials, including nanoparticles, nanowires,

and Two-dimensional (2D) materials, will be discussed and compared with bulk oxidation. Our review would provide a systematic overview of the central role of computational techniques in probing the atomic-scale oxidation mechanisms, which are ceaselessly offering theoretical guidance to the synthesis of cutting-edge oxide-based materials.

2. Computational techniques for atomistic simulations of oxidation

Before the invention of computers, most scientists conducted experiments or theoretical analysis to understand the structures and properties of materials. Using modern computational techniques, we are now able to predict the structure–property relation of an unknown material prior to the experimental discovery, evaluate their dynamic behaviours under a physical process or chemical reaction, and design novel materials in a high-throughput way.

With the staggering development of computer hardware, QM theories, and modern algorithms, computer modelling has become an indispensable part of materials science research to interpret, guide, and predict experiments. The field of computational materials science is now integrated with various modelling techniques at multiscale. Several representative modelling methods are listed in Fig. 1 with their suitable ranges of applications. In general, one of the most prominent features of computer modelling is that increasing the time or length scales usually results in the loss of computational accuracy. There is no single technique that can cover all the time and length scales within reasonable computational times, and each method has its expertise in solving particular problems. Next in this section, some typical computational techniques will be elucidated according to the order of modelling scale, from the tiny one to the larger.

Electronic structure techniques allow us to accurately anticipate the structures and properties of most materials. However, the full QM description of multi-electron systems is too complex and approximations must be included in such calculations. Therefore, QM calculations are usually performed in systems with less than hundreds of atoms to predict the ground-state structures and properties of materials. Calculations based on the DFT [31,32] and transition state theory [43] further enriched their applications in chemical reactions. DFT has become a standard tool that is widely used by numerous researchers in various disciplines. However, DFT still has limitations due to its mathematical complexity. Traditional DFT calculations correspond to zero-temperature and zero-pressure conditions. *Ab initio* thermodynamics extend DFT results to the finite temperature and pressure conditions encountered in experiments based on free energy calculations, which are particularly useful for predicting surface structure stability under reaction conditions [44–46]. At the current stage, calculations of tens of atoms are routine, and hundreds of atoms or more are possible on high-performance computing (HPC) platforms. However, researchers are always interested in probing complex materials, macromolecules, defects, and multiphase interfaces, as well as their dynamic behaviours far away from the equilibrium states. Therefore, computational materials science starves for methods suitable for larger scale, in response to which MD simulation emerges at the exact moment.

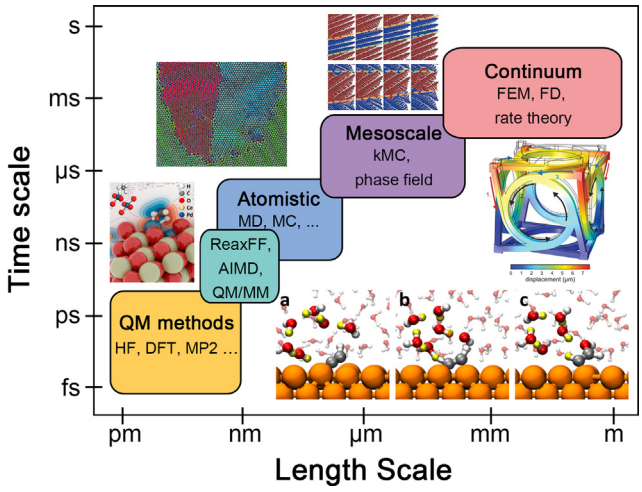

Fig. 1. Computer modelling methods in materials science at different time and length scales [38–42].

Based on interatomic potentials, MD simulation [33] can be employed to obtain the trajectories of multi-atomic systems under a physical or chemical process, dealing with thousands, millions, even billions of atoms [47], ranging from femtosecond (fs) to microsecond (μs) [48] in the time scale. MD simulation calculates the real-time trajectories of multiple interacting particles during a dynamic process, enabling one to visualise the atomic motion *in silico*. It is a versatile tool with broad applications in areas such as materials science, condensed matter physics, chemistry, biology, and pharmacy. In materials science, we can employ MD simulations to anticipate the structures and properties of materials at the equilibrium state, as well as investigate the dynamic phenomena that happened inside or on the surface of materials, such as diffusion [49,50], phase transition [51], interfacial phenomena [52], and defect dynamics [53].

In recent years, MD simulation has become increasingly mature. A variety of open-source packages for both performing and visualising MD simulations have been developed. The development of new types of interatomic potentials such as the charge transfer ionic potential (CTIP) potential [54] and reactive force field (ReaxFF) [55,56] has extended the scope from purely physical systems to reactive systems. The establishment of HPC platforms and GPU acceleration algorithms has led to the successful modelling of mesoscale systems containing billions of atoms [47,57]. Genetic algorithms, deep learning, and machine learning (ML) techniques have created new paradigms to develop advanced interatomic potentials with improved accuracy [58–60]. MD simulation has revolutionised the research work in materials science and is keeping contributing to addressing the key problems from an atomic-scale perspective.

Traditional force fields cannot model chemical reactions because of the lack of an appropriate description of the chemical bond forming and breaking in a reactive event. The development of the ReaxFF is targeted at this limitation and has successfully helped bridge the gap in the simulation scale (Fig. 1) by explicitly describing the bond activity and charge transfer. The ReaxFF method was initially proposed by van Duin [55] in 2001 to model hydrocarbon reaction, which has now been extended into a wide range of reactive systems. The application of the ReaxFF MD simulations (ReaxFF-MD or RMD) enables one to monitor the dynamic evolution of a reactive system at the atomic scale, with broad applications as wide range as oxidation, reduction, corrosion, heterogeneous catalysis, conformational dynamics of biomolecules, and liquid–solid interfacial phenomena [56,61–67]. Many ReaxFFs have been developed targeting at studying the atomic-scale oxidation of materials, such as carbon materials [68], Si [69,70], SiC [71], SiO_2 [72], Si_3N_4 [73], Pd [74], Pt [75,76], Ni [77], Cr [78], Al [79,80], Ge [81,82], Fe [83], Cu [65], Ag [84], Au [85], MoS_2 [86], and Mxenes [87]. The ReaxFF-MD simulation has been implemented in the open-source LAMMPS code [88]. ReaxFFs can also be applied to grand canonical Monte Carlo (GCMC) simulations for predicting the structure and phase stability of materials under reaction environments [89–92]. ReaxFF-based nudged elas-

Table 1
Recent advances in modelling atomic-scale oxidation of materials using various computational approaches.

System	Research focus	Computational approaches	Ref.
Fe nanoparticles	Formation of hollow oxide nanostructure	ReaxFF-MD	[19]
Si, bulk and nanowires	Dynamical oxidation mechanism	ReaxFF-MD	[104]
Al/graphene oxide	Ignition and combustion	ReaxFF-MD	[105]
Al, bulk	Formation of oxide bifilms	ReaxFF-MD	[106]
Ti_3C_2 MXene	Environmental effects in oxidation	ReaxFF-MD	[107]
Al nanoparticle (ANP)	Structural evolution during oxidation	ReaxFF-MD	[108]
Nb, bulk	Oxygen embrittlement	MD + DFT	[109]
Ag(111) and Ag(001)	Ag-O and Ag-S reactions	ReaxFF-MD + DFT	[110]
Ta, bulk	Force-field development	CTIP-MD	[111]
Cu-Hf alloy	Force-field development	CTIP-MD	[112]
Si, bulk	Amorphous-structure-promoted oxidation	ReaxFF-MD	[93]
Graphene	Effects of defects in oxidation	ReaxFF-MD	[96]
ZrS_xSe_{2-x} and MoS_2	Dynamical oxidation mechanism	ReaxFF-MD + DFT	[113]
$Ti_{n+1}C_n$ Mxenes	Dynamical oxidation mechanism	ReaxFF-MD + DFT	[95]
Cu nanoparticles	Dynamical oxidation mechanism	ReaxFF-MD	[114]
Diamond surfaces	Hummer's method	ReaxFF-MD	[115]
Cu(111)	Corrosion inhibitor molecules	ReaxFF-MD + DFT	[116]
Carbon fibre and char	Dynamical oxidation mechanism	ReaxFF-MD	[117]
Pt(111)	Oxide film growth	ReaxFF-GCMC	[92]
Ag(111)	Surface phase diagram prediction	ReaxFF-GCMC	[118]
Pt nanoparticles	Degradation of Pt nanoparticle electrocatalysts	ReaxFF-GCMC + ReaxFF-MD + DFT	[91]
Pt nanoparticles	Oxygen adsorption on high-index facets	ReaxFF-GCMC + ReaxFF-MD	[119]
ZnO	Stability of polar oxide surfaces	DFT + MC	[120]
Ag(110)	O_2 dissociation and adatom extraction	DFT	[121]
Wurtzite AlN(0001)	O_2 adsorption mechanism	DFT	[122]
Ni-Cr alloy	Water-vapour-promoted oxidation	DFT	[123]
Mg	Electrochemical corrosion	DFT	[124]
Au(111)	K atom promotion of O_2 chemisorption	DFT	[125]
Cu, bulk	Surface modifcations for anti-oxidation	DFT	[25]
Nanotwinned Ag and Pd	Site-selective effects of stacking-faults and twin boundaries in oxidation	DFT	[126]
Si, bulk	Oxygen segregation in grain boundaries	DFT	[127]
Cu(100)	Unusual layer-by-layer growth mechanism	DFT	[128]
Cu nanoparticles	Non-oxidised state with excess electrons	DFT	[30]
Mg-Ca alloy	High-temperature oxidation mechanism	DFT	[117]
Pd(100) and Pd(111)	O_2 dissociation and Hot adatom diffusion	DFT + AIMD	[129]
Al(111)	Oxidation protection with amorphous surface oxides	DFT + AIMD	[130]
$CH_3NH_3PbI_3$	Effects of surface superoxide/peroxide	DFT + AIMD	[26]
$Fe_{0.28}Co_{0.21}Ni_{0.20}Cu_{0.08}Pt_{0.23}$ high-entropy alloy nanoparticles	Dynamical oxidation mechanism	DFT + AIMD + MC	[131]
Cu clusters	Oxidation and cluster fluxionality	DFT + AIMD	[132]
CeO_2	Stability of polar oxide surfaces	DFT + *ab initio* thermodynamics	[133]
TiO_2	Predicting monolayer oxide stability	DFT + *ab initio* thermodynamics	[134]
Ir surfaces	Oxide stability and catalytic activity	DFT + *ab initio* thermodynamics	[135]
W_5O_{14} and $W_{18}O_4$	Phase stability under gas- and solution-based synthesis environment	DFT + *ab initio* thermodynamics	[136]
Pt(111)	Thermodynamics of PtO_2 stripe formation	DFT + *ab initio* thermodynamics	[137]
Cu, bulk	Multiple environmental factors in oxidation and corrosion	DFT + *ab initio* thermodynamics	[138]
Cu(111)	Early stage oxidation mechanism	DFT + *ab initio* STM simulation	[139]
Monolayer metal oxides	Descriptor discovery	DFT + ML	[140]
Cu nanoclusters	Structural evolution during oxidation	DFT + grand canonical basin hopping (GCBH)	[141]
Al(111)	Activation barrier for O_2 dissociation	DFT + Embedded correlated wave function (ECW)	[142]

tic band (NEB) calculations can be used for finding the transition states and minimum energy paths in the reactions [75,93–96]. Additionally, charge-optimised many-body (COMB) potential is another force field employing the bond order dependent approach and has been adapted to several metal-oxide systems [97–99].

At larger scales, MC [100] techniques could further extend the simulated systems to the mesoscale. In macroscale modelling, atoms are no longer viewed as the basic constitutional unit. Instead, continuum-based methods such as phase-field simulation [101] and finite element modelling (FEM) [102] play more important roles in solving industrial problems, such as alloy solidification, materials forming, and welding. Machine learning technology has recently established an entirely new framework to quickly and efficiently screen for new materials with desired properties and functions [103]. The cross-fertilisation of different computational techniques provides valuable solutions to fundamental materials science and engineering problems, which has substantially accelerated our understanding of solid-state science and contributed to the development of cutting-edge materials. In Table 1, we summarised the recent advances over the past few years in modelling the oxidation mechanisms of solid materials using various computational approaches.

3. Overview of oxidation of bulk materials at the atomic scale

3.1. Cabrera-Mott theory

Many solids get oxidised, rusted, burned or decomposed when exposed to air or water since antiquity. In the 19th century, scientists began to realise that these phenomena stem from the rearrangement of surface atoms driven by chemical reactions. Scientists had always dreamed of observing these phenomena at

an atomic level in real-time. However, the resolution of characterisation techniques is not high enough to this dream up to date. Theorists also proposed several physical models to describe the oxide growth phenomena. One of the most well-known theories was proposed by Cabrera and Mott [1] in 1949, which solved the problem of the kinetics and driving force of the low-temperature oxide film growth on metal surfaces.

Fig. 2 shows the schematic diagram of the Cabrera-Mott model. Fig. 2a-b illustrates the positions of electronic levels in the metal, oxide, and adsorbed oxygen layers before and after the equilibrium. The primary assumption of this model is that electrons can freely ionise the adsorbed oxygen atoms/molecules, resulting in a uniform electric potential in the growing oxides. This electric potential is called Mott potential V_M, which is established by the negatively charged oxygen anions and the positive surface charge of the metal. Because the thickness of the oxide film x is rather small at the initial stage of oxidation, the electric field $F = V_M/x$ can be very strong [1]. In the Cabrera-Mott theory, oxide growth proceeds by cation migration between the interstitial sites at the metal/oxide interfaces. The initial migration to cross the metal/oxide interface requires an activation energy W, which is much higher than the subsequent migration barrier in the oxide layer, as the potential energy diagram shown in Fig. 2c. The Mott potential significantly reduces the migration barriers by $1/2qaF$, where q is the atomic charge, a is the jump distance between two interstitial sites. Consider the Arrhenius relation between rate constant k and barrier.U

$$k = Aexp\left(-\frac{U}{k_BT}\right) \tag{1}$$

where A is the Arrhenius constant, k_B is the Boltzmann constant, T is the temperature. The oxidation rate is significantly enhanced when the barrier is reduced.

Cabrera and Mott also proposed that the rate-determining process for the oxide film growth is the introduction of point defects at the metal/oxide or oxide/gas interfaces because this process has the highest activation barrier. This is divided into two situations, as shown in Fig. 2d-e. When a defect is injected at the metal/oxide interface (Fig. 2d), it can be an interstitial metal ion or an oxygen vacancy. For example, the reaction for the former type can be described as: $M_{(metal)} \rightarrow M^{\dot{A}\cdot\dot{A}\cdot}_{i(oxide)} + 2e'_{(metal)} + V_{(metal)}$. Due to the existence of the Mott potential, the migration barrier is lowered by $1/2qaF$, and the velocity for the cation migration becomes.

$$k = Aexp\left(-\frac{U}{k_BT}\right)\exp\left(\frac{qaF}{2k_BTx}\right) \tag{2}$$

The rate of oxide film growth is then given by.

$$\frac{dx}{dt} = \frac{D_i}{a}exp\left(\frac{qaF}{2k_BTx}\right) \tag{3}$$

where D_i is the atomic diffusion coefficient. Define $x_1 = qaF/2k_BT$. When the oxide film thickness x is much smaller than its limiting thickness x_L, we obtain the inverse logarithmic rate law for the oxide film growth.

$$\frac{x_1}{x} = -ln\left[\frac{D_i x_1 t}{a{x_L}^2}\right] \tag{4}$$

When a defect is introduced at the oxide/gas interfaces (Fig. 2e), the defect type can be the metal vacancy or oxygen interstitial. The defect reaction for the formation of metal vacancy is: $M^{\times}_M + O''_{(surface)} \rightarrow V^{\dot{A}\cdot\dot{A}\cdot}_M + MO$. Only the metallic cations that combine with surface O^{2-} anions within one jump can participate in this reaction. Therefore, the oxide growth rate is determined by the average coordination number N of metallic ions with oxygen, which is given by.

$$\frac{dx}{dt} = \frac{N\varepsilon\varepsilon_0 F}{2eN_s x}\frac{D_i}{a}exp\left(\frac{qaF}{2k_BTx}\right) \tag{5}$$

where ε and ε_0 are the dielectric constants for the metal and vacuum, e is the modulus of the electronic charge, N_s is the total number of ions per unit surface area. The limiting thickness of the oxide film, in this case, is smaller than the first one.

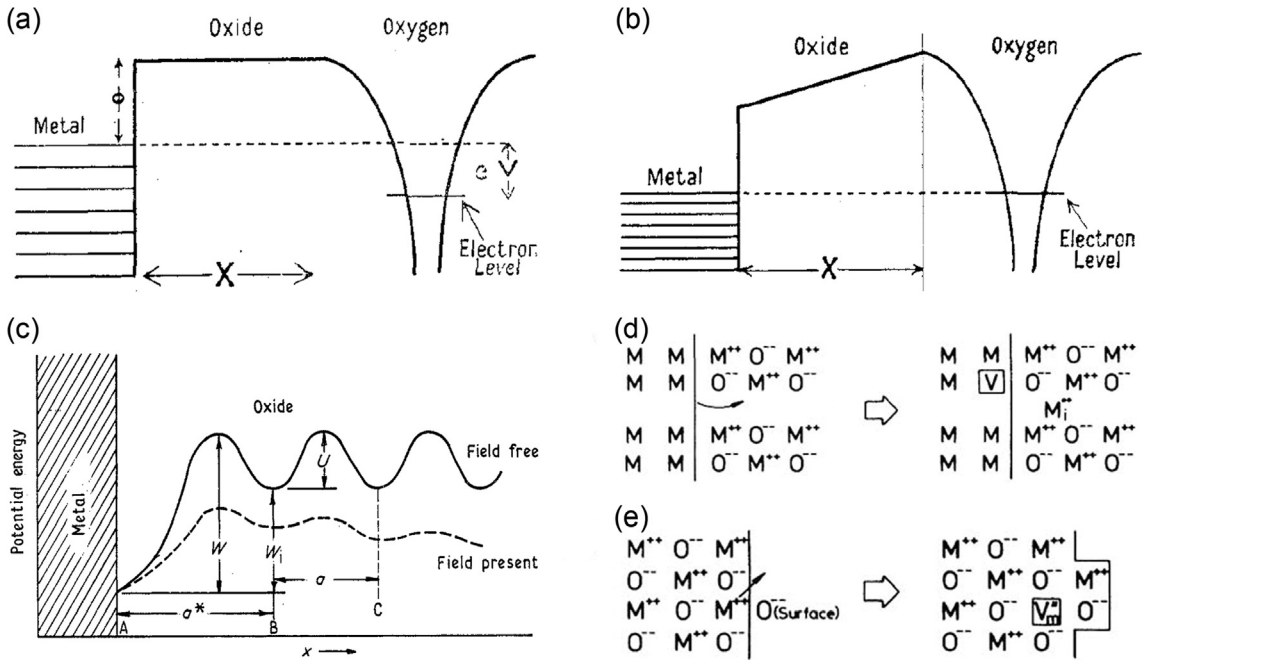

Fig. 2. The Cabrera-Mott model. (a) The electronic levels before the electrons have passed through the oxide. (b) The electronic levels when the equilibrium state is reached. (c) Potential energy barriers for cation migration with and without the presence of electric field. Possible reaction pathways for the point defect migration (d) At the metal/oxide interface and (e) at the oxide/gas interface [1,143,144].

In addition to the Cabrera-Mott theory, there are also plenty of kinetic models proposed for describing the oxide film growth [144]. It is vital to understand that oxidation of metals is a complex physicochemical process and can be affected by various intrinsic (local atomic structure, chemical composition, defects, and impurities) and environmental factors (temperature, pressure, humidity, and external fields). Each kinetic model may only be used to describe the oxidation of a limited range of metals in a particular reaction environment. Using *in situ* observation techniques and modern computational modelling methods, we are now able to visualise the atomic rearrangement during oxidation. The combination of experimental and theoretical techniques has been unceasingly improving our knowledge, fabricating new theories, and accelerating industrial production.

3.2. Modelling solid-oxygen interactions and the oxide film growth

The oxidation of general materials can be divided into two stages. In the initial stage, the incorporation of oxygen atoms results in the rapid formation of a monatomic layer of 'pseudomorphic' oxide (usually <1 s) [1]. Afterwards, the oxide film slowly grows steadily and eventually reaches the limiting thickness, which could last several days. The second stage is controlled by the rate of some basic physical and chemical steps, such as ion migration, electron transport at the interface, or electron transfer during the chemisorption. Cabrera-Mott theory that describes the oxide film growth actually focuses on the second stage.

At the beginning of oxidation, oxygen molecules first adsorb on the surface and dissociate or partially ionise. The dissociated oxygen atoms then undergo surface reconstruction by diffusion [143]. The adsorption energy E_{ad}, which is the key property to describe the adsorption process, is defined as.

$$E_{ad} = E_{solid-gas} - (E_{solid} + E_{gas}) \quad (6)$$

where $E_{metal-gas}$ is the energy of the bound complex after adsorption, E_{solid} and E_{gas} are the energies of the isolated slab and gas molecule, respectively. According to this definition, a positive value indicates that the adsorption process is endothermic, while a negative value represents an exothermic process. Nørskov and co-workers have established a widely accepted *d*-band centre theory based on DFT calculations that demonstrates the linear relationship between the activity of transition metal surfaces, adsorption energy, and electronic structures [145–147]. Based on this theory, the strength of O adsorption on transition metal surfaces is solely determined by the position and width of metal *d*-states in the energy levels [146,148]. Therefore, the resistance to oxidation and catalytic activity of metal or alloy surfaces can be accurately predicted and quantified using DFT calculations. The adsorption of O_2 on metal surfaces is coverage-dependent. The adsorption energy of O_2 on metal surfaces usually exhibit a rising trend with the increase in coverage due to the repulsive nature of the adsorbate–adsorbate interactions [149]. Therefore, as the oxide film grows, the heat supplied by oxygen adsorption gradually decreases that finally cannot overcome the reaction barrier, resulting in a limiting thickness of the oxide film [4]. In addition, the adsorption energy is also sensitive to surface defects. The O atoms could interact with metal atoms more strongly when vacancies are introduced [150].

Many experimental observations confirmed that oxidation-derived thin oxide films formed on many types of bulk materials (Al, Zn, Fe, Cr, Zr, Ti, Ta, Si etc.) have a 'pseudomorphic' form as illustrated by Cabrera and Mott [1]. The term 'pseudomorphic' were further known as 'amorphous' [151], suggesting that these oxide films do not have periodically repeated units in their atomic structures, which is different from the thermodynamically more stable crystal oxides. Conventionally, it is known that amorphous structures have higher energy than their crystalline counterparts with the same type of components. Why do the surface oxide films prefer to have a metastable amorphous structure? The formation of amorphous structures has long been regarded as a kinetic phenomenon. For example, liquids can solidify in two different ways. Crystalline structure with long-range order is formed at low cooling rates, while metastable amorphous structures without long-range order can be formed at high cooling rates [152–154]. However, the formation of surface amorphous oxides is in another picture. Jeurgens *et al.* [155–157] proposed a thermodynamics framework to clarify that the formation of amorphous oxides on surfaces is actually controlled by thermodynamics (Fig. 3a). While amorphous oxide films have higher bulk Gibbs energy, the energy difference with crystal structures can be compensated by the more negative surface and interface energies within a certain critical oxide-film thickness. The critical thickness is dependent on the materials types and surface orientation. Moreover, when the oxide film grows beyond the critical thickness, large activation energy is still required to complete the amorphous-to-crystalline transition so that the oxide film retains the amorphous phase. This conclusion is verified in our recent ReaxFF-MD study on the oxidation of silicon, in which a very high temperature (greater than1500 K) is needed to initiate the crystallisation of the amorphous surface oxides [93]. Recently, Aykol and Persson [130] combined DFT and AIMD calculations to illustrate the initial phase selection during the oxide growth on the Al(1 1 1) substrate. The optimised configurations of the oxide films with different thicknesses composed of the corundum (α-Al_2O_3), spinel (γ-Al_2O_3), and amorphous (am-Al_2O_3) structures are shown in Fig. 3b. It is concluded that when the oxide film is less than 1 nm, the amorphous structure is the most stable phase; when the thickness is greater than 1 nm, the γ phase becomes more stable; the most stable phase of bulk alumina has the α-corundum structure (Fig. 3c). In addition, the atomic structure of the γ-phase oxide film on the Al (1 1 1) substrate is highly distorted, with randomly distributed four-coordinated and five-coordinated Al-O polyhedron units (compared with an ordered mixture of four-coordinated and six-coordinated Al-O polyhedrons in bulk γ-Al_2O_3). The close-packed O framework is lost, and the structure becomes nearly "amorphous-like" (Fig. 3b). This work provides a quantitative understanding of the structural evolution rules in the growing oxide films.

Materials are not always perfect at the atomic scale, with various structural defects such as vacancies, interstitials, dislocations, grain boundaries, and step edges. The formation energies of those defects on the surfaces are usually lower than in bulk, which could become the active sites and change the oxidation mechanisms. Many computational studies have indicated that oxidation mechanisms and kinetics are highly correlated with the local disordered structures in materials such as vacancies [77,109], grain boundary [110,127,158], step edge [64,128,159], nano-trench [160], alloying [112], and amorphous structure [93]. Computational studies revealed that O atoms are strongly coupled with the vacancy sites and voids in metals which significantly facilitate the inward diffusion of O atoms during oxidation [77,109]. The ReaxFF-MD simulations performed by Zou *et al.* [77] showed that oxygen ions spontaneously diffused and gathered near the voids in bulk Ni, which initiated the oxide nucleation. Grain boundaries are also known as a key promoter to the oxidation process, which is one of the main causes of intergranular embrittlement [96,110,126,127,161,162]. External factors on the oxidation kinetics were also studied, such as temperature [104], pressure [108], external fields [2,16], and humidity [123].

Step edge is a common defect that usually exists between different facets, especially on the surfaces of nanomaterials. On the step edges, under-coordinated atoms are piled up into terrace-

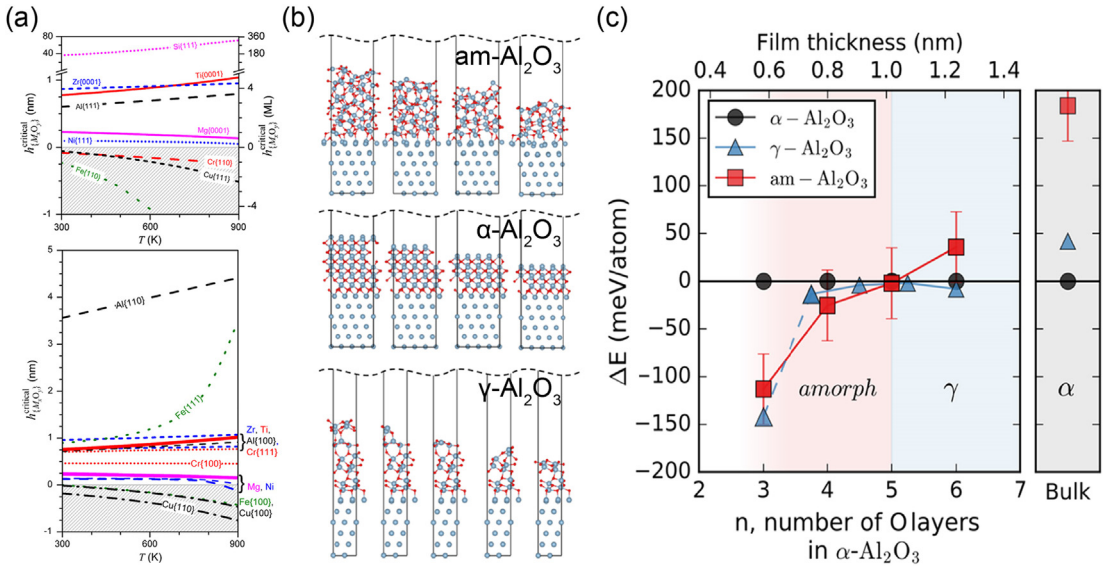

Fig. 3. Phase selection of the growing oxide films on solids. (a) The critical thicknesses for the amorphous-to-crystalline transition of surface oxide films at various temperatures predicted by a thermodynamic model. (b) The optimised morphologies of the Al(1 1 1) substrate covered with different layers of am-Al_2O_3, α-Al_2O_3, and γ-Al_2O_3 films. (c) Energy of the oxide films on the Al(1 1 1) substrate with respect to the α-Al_2O_3(0001) film as a function of the number of oxide layers [130].

like surfaces. Yang *et al.* [64,128,159,163–167] combined *in situ* environmental transmission electron microscopy (ETEM) observations with modern computational techniques to study the early-stage oxide nucleation and growth on Cu stepped surfaces. An unusual layer-by-layer growth mechanism of Cu_2O nano-island was found due to the existence of surface steps that contradicts to classical theories (Fig. 4a-g) [128]. Oxidation of stepped Cu surfaces through the formation and growth of Cu_2O islands on flat terraces. After the formation of islands, the dissociation of O_2 on Cu is no longer energetically favourable, which transfer to Cu_2O surfaces and supply diffusing O atoms (Fig. 4e). The surface steps then become the source of Cu adatom diffusion that drives the formation of Cu_2O islands (Fig. 4f), which could bypass the normal reconstructive adsorption or subsurface oxygen incorporation, resulting in flattened metal-oxide interfaces [128,163]. When surface steps are far away, Cu adatom will also be transported through the vacancy-assisted interfacial diffusion (Fig. 4g). DFT calculations and ReaxFF-MD simulations revealed that the facet-orientation-dependent adsorption energy and oxygen diffusion barrier are the key determinants of the oxide growth kinetics and quality [64]. Several kinetic and thermodynamic descriptors were proposed based on computational methods for predicting the oxide growth preferences on stepped surfaces [64,165,167]. Recently, they further bridged experiments and modelling to demonstrate the uneven oxidation kinetics and surface reconstructions at the surface steps [128]. It is concluded that Cu(1 0 0) strongly favours the oxidation of upper terraces, while the preference on Cu(1 1 0) depends on the oxygen concentration, as shown in Fig. 4h-j [167]. These accomplishments are of great importance for advanced science, such as anti-corrosion oxide film design, Cu-based catalyst optimisation, and oxide nanodevice manufacturing [168].

Computational methods such as DFT calculations and ReaxFF-MD simulations are suitable to understand the early-stage oxygen chemisorption and oxide nucleation mechanisms, while *in situ* microscopies can further provide information on the later-stage oxide growth kinetics. In recent years, the progress of developing reliable interatomic potentials has been substantially accelerated by novel algorithms such as machine learning, neural network, genetic algorithms, and deep learning techniques [60,169–172], which will undoubtedly promote the atomic-scale exploration of more complex systems modelling oxidation, corrosion, and other interfacial reactions. Experimental and theoretical approaches working in tandem have significantly boosted our understanding of the atomic-level mechanisms throughout the oxidation processes, which is the key to the precise control of oxide nanostructures for functional applications [19,30,123].

4. Modelling oxidation mechanisms of nanomaterials

4.1. Oxidation of nanoparticles: Formation of various nanostructures

As nanomaterials often show new and unexpected features, oxidation of nanomaterials often has unique characteristics with complex mechanisms. Oxidation of nanoparticles can result in a diversity of nanostructures. The most common configuration is the core–shell structure (Fig. 5a). By utilising computational approaches, the formation of the oxide shell on the nanoparticles could be delicately observed in real-time. Cabrera-Mott model can be applied to describe the oxide shell growth kinetics [173]. Importantly, the morphology, adhesion, composition, and porosity of the oxide shell depend on various intrinsic factors of nanoparticles such as the expansion ratio of materials caused by the insertion of oxygen atoms, the reactivity and diffusivity of the inherent elements, the initial geometry and surface structure of the nanoparticle, which could all be demonstrated by simulations. Fig. 5b shows the 3D structure evolution during the oxidation of Fe nanoparticles, in which the upper figures are reconstructed from experimental SAXS patterns while the bottom figures are from ReaxFF-MD simulations [19]. In contrast to the formation of core–shell structure in Fig. 5a, the oxidation of Fe nanoparticles is a nanoscale Kirkendall process—the formation, growth, and coalescence of small voids inside the Fe nanoparticles, which transforms the solid nanoparticles into hollow oxide nanoshells. This study suggests that defect formation and clustering play a critical role in determining the formation of oxides on nanomaterials. It is concluded that in a diffusion-limited oxidation mechanism, when the oxygen atoms in the oxide layer diffuse faster than the inherent atoms, the nanoparticles will grow into a core–shell struc-

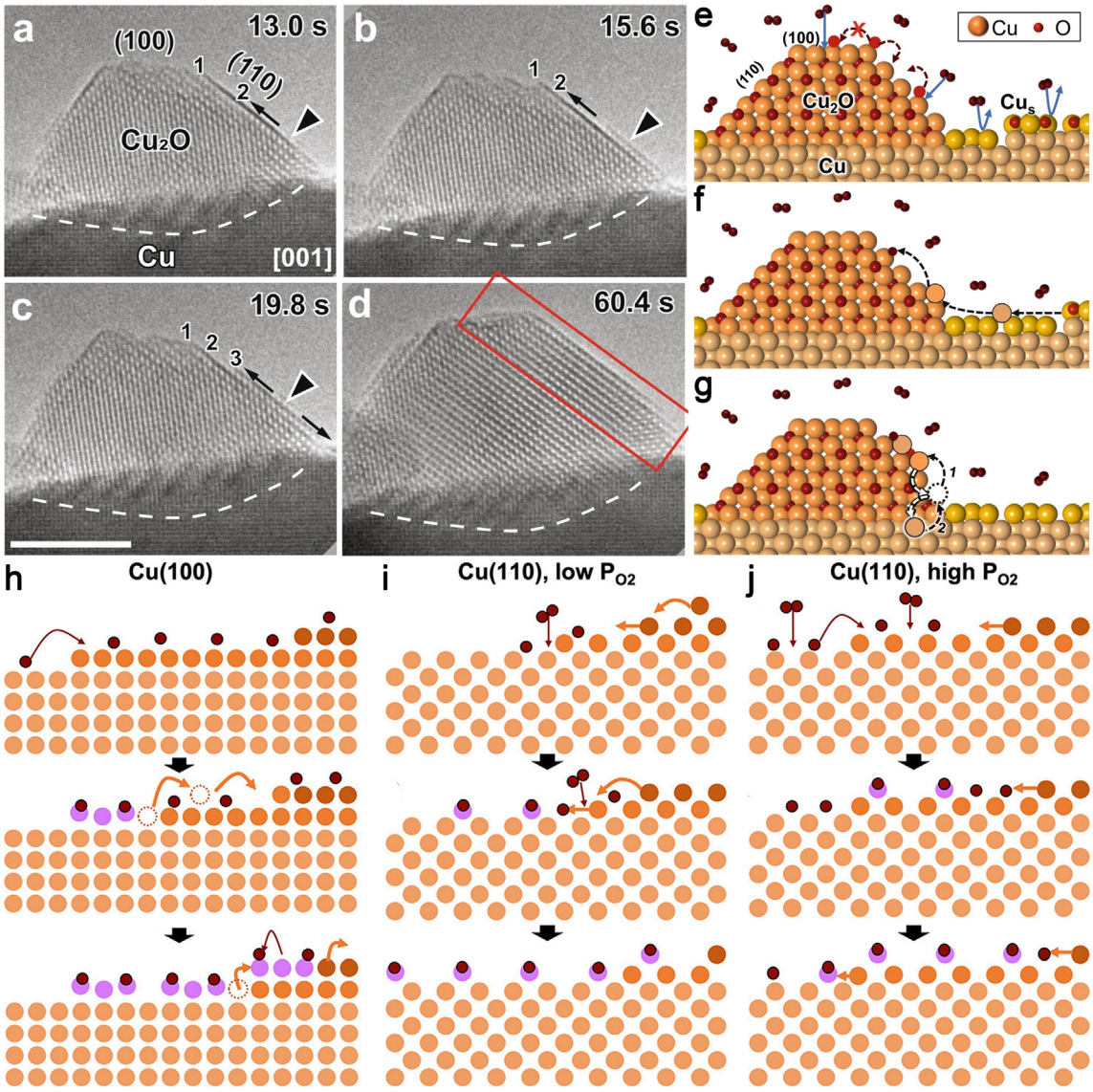

Fig. 4. Combining experiments with theoretical calculations to study the dynamic processes of oxide growth on Cu stepped surfaces. (a-d) ETEM observations of the layer-by-layer oxide growth along $Cu_2O(1\,1\,0)$ during Cu(100) oxidation. The layer nucleation site (triangle) and growth direction (arrow) are indicated. Scale bar: 5 nm. (e-g) Schematic of Cu_2O growth mechanism which demonstrates the role of surface steps on (e) the dissociation of O_2, (f) Cu adatoms diffusion, and (g) vacancy-mediated interface diffusion of Cu atoms. (h-j) Schematic of surface reconstruction on Cu(1 0 0) and Cu(1 1 0) surfaces affected by surface steps and O_2 concentration [128,167].

ture, just as the case in Fig. 5a. On the contrary, when the diffusion of inherent atoms is faster, the overall mass transportation is outward so that voids will be formed at the interface through the Kirkendall effect (Fig. 5b). Kirkendall effect was first observed in 1947 in bimetallic bulk diffusion couple [174], which revealed that the difference in the diffusivity of metals could lead to the formation of voids at the interface and further drive the interface immigration. Conventionally, Kirkendall effect is detrimental to the mechanical properties of alloys, which should be overcome in metallurgical engineering. However, at the nanoscale, Kirkendall effect is valuable in preparing nanocrystals with hollow or yolk-shell structures, which have broad prospects in the field of energy storage and conversion, such as lithium-ion batteries, supercapacitors, solar cells, and photocatalysis [175–177].

On the surface of oxidised nanoparticles, large local strain fields favour the formation of unstable metal/oxide interfaces that are hard to relax [178]. Pratt *et al.* [179] reported an interesting morphological change during the oxidation of cuboid Fe nanoparticles under atmospheric conditions, which highlights the effects of strain in determining the structure and morphology of the oxidised products. As shown in Fig. 5c, the Fe nanoparticle changes from cuboid to spherical first, which is caused by the strain-gradient-enhanced ionic transport at the nanoparticle surface. Compared with the corner regions, the central regions of the cube surface have a higher oxidation rate because the lattice mismatch at the oxide/oxide interface results in a positive strain gradient that modifies the nanoparticle shape. Finally, the fully oxidised nanoparticle generates a Kirkendall void in the centre, which is consistent with Sun *et al.*'s work [19].

The structures of hollow oxide nanoparticles formed by the Kirkendall effect can be more complex in some conditions. A recent *in situ* experimental study performed by Xia *et al.* [22] revealed the structural evolution of a bimetallic Ni_xFe_{1-x} nanoparticle with variable Ni/Fe ratios. As shown in Fig. 5d, three types of oxidised morphologies, namely, hollow structure, dual-cavity structure, and porous structure, can be formed at different initial Ni/Fe ratios. Lower Fe concentration leads to more porous oxide structures in this system, which is attributed to the difference in the diffusivity

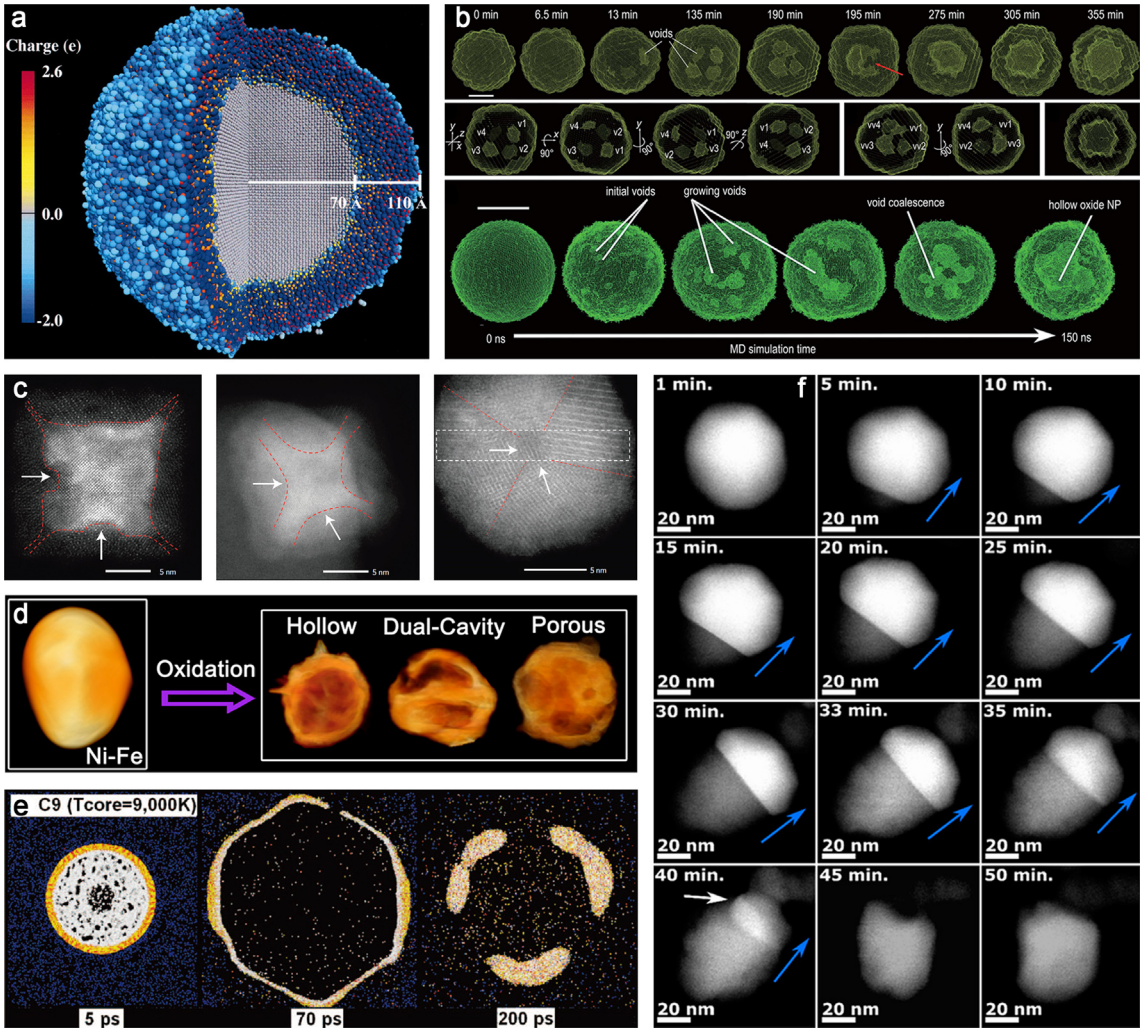

Fig. 5. Complex structural evolution processes of nanoparticles during oxidation. (a) The formation of core–shell structures in the oxidation of aluminium nanoparticles. (b) Hollow nanostructures produced by the oxidation of iron nanoparticles. (c) Oxidation-induced structural transformation from cuboid to spherical of iron nanoparticles. (d) The porosity of the oxidised Ni-Fe bimetallic nanoparticles is closely related to the reaction condition. (e) Explosion of aluminium nanoparticles under extreme conditions. (f) Oxidation of copper nanoparticles in an interface-migration regime [19,22,179,181–183].

of Fe and Ni. This study also emphasises the size effect of nanoparticle oxidation: larger nanoparticles prefer to form porous structures, while smaller ones favour hollow structures. The similar structural complexity of oxidised nanoparticles is also shown in the Ni-Co system [180].

Recently, by utilising ReaxFF-MD simulations, we employed the Al/O ReaxFF to develop a comprehensive understanding of the oxidation mechanism of ANPs, paying particular focus on the effects of reaction conditions and nanoparticle size on the structure evolution [108]. Our computational work elucidated a distinct chain-like oxide nucleation and growth mechanism on ANPs induced by a synergistic effect of surface active sites, heat release by oxidation, and internal stress. The outstanding reactivity of nanoparticles is correlated with the abundant active sites on the surface, which play a pivotal role in chemical reactions. Fig. 6 shows the atomic arrangement of an ANP with a diameter of 5 nm. The surface of the ANP is composed of several smooth facets and surface steps. On the surface steps, the atoms have much smaller coordination numbers than those on the facets, which serve as the active sites for the dissociative adsorption of oxygen molecules [184,185].

ReaxFF-MD simulations enable us to predict the oxide growth patterns on ANPs in different reaction conditions. In general, there are three types of oxide growth patterns: formation of the oxide shell, outward growth of chain-like oxides, and explosion into oxide clusters, which is shown in Fig. 6b-d. The oxidation rate on the stepped facts is significantly faster than that on the smooth facets (most of them are Al(1 1 1)), which is consistent with previous observations of the very low dissociative sticking probability of O_2 on Al(1 1 1) [186]. Through statistical thermodynamics calculations, we uncovered the origin of this interesting phenomenon. As introduced above, the formation of Al-O bonds could release a large amount of heat and perturb the surface atomic structure. In the ANP system, the oxidation reaction is rather rapid so that the heat concentrates on the surface without transferring to other places. Calculations showed that there is a temperature gradient inside the ANPs during the oxidation, where surface Al atoms have much higher kinetic energy than the inner atoms. The kinetic energy gradient along the radius of heated nanoparticles is a universal phenomenon. Liu *et al.* [187] recently proposed that the atoms at the corner and edge sites could attain higher kinetic energy than other atoms when the nanoparticle is heated. A similar high reactivity of the edge and corner atoms is also observed in methane oxidation catalysed by Pt nanocrystals [188]. As a result, the increased kinetic energy of surface atoms induces structural expansion and internal stress, which drive the surface oxides and some Al atoms to move outward and form atomic chains. In some extreme condi-

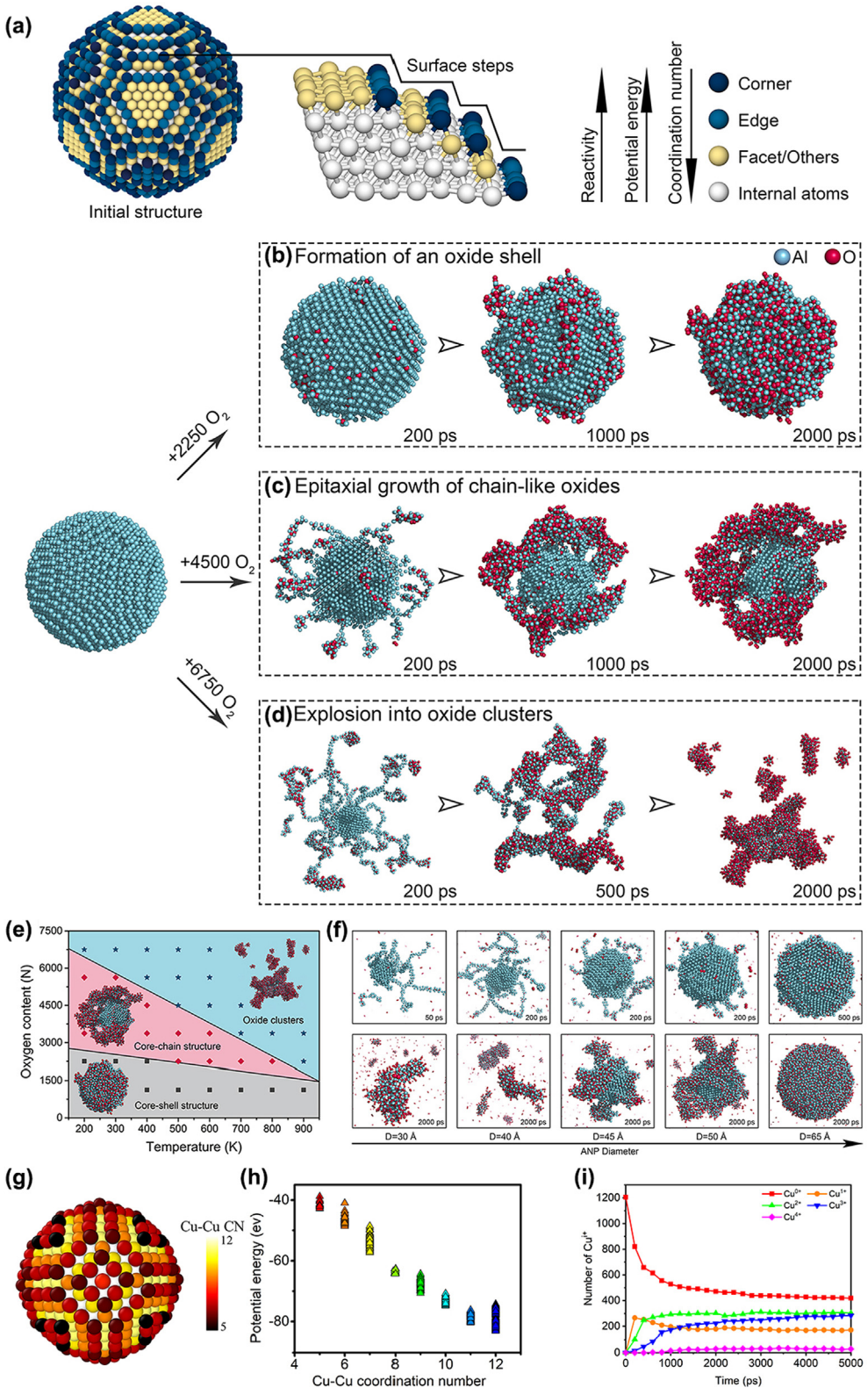

Fig. 6. Oxidation of Al and Cu nanoparticles simulated by the ReaxFF-MD approach. (a) Active site distribution on an ANP with a diameter of 5 nm. Atoms are coloured to reflect their coordination environment [108]. ReaxFF-MD simulations of the oxidation of ANPs. Three types of oxide growth patterns are observed, which are: (b) formation of an oxide shell, (c) outward growth of chain-like oxides, and (d) explosion into oxide clusters. (e) The relation between the morphology of the oxidised products of the ANP with a diameter of 5 nm and reaction conditions. (f) Size effect of the oxidation of ANPs under the same reaction condition. Colour code: cyan, Al; red, O. (g) The initial morphology of Cu NP. All the atoms are coloured according to the Cu-Cu coordination number. (h) The potential energy distribution of all Cu atoms according to their Cu-Cu coordination number at 300 K. (i) The evolution of different coordinated structures of Cu in the condition of 3000 O_2 contents at 300 K [108,114]. (For interpretation of the references to colour in this figure legend, the reader is referred to the web version of this article.)

tions, the ANP explode drastically into many rough and irregular oxide clusters, as shown in Fig. 6d. The small oxide clusters could also merge into larger ones in their collision. We further performed oxidation simulations of ANPs at various temperatures and with different initial oxygen contents, which comes to the conclusive diagram about the correlation between the morphology of the oxidation products and reaction conditions (Fig. 6e). The simulations predicted that the oxidation products have three types of morphologies: core–shell structure, core-chain structure and oxide clusters [108,189]. Such complex morphological evolution is also observed in the reactions of Al and AlH_3 nanoparticles with other reactants such as H_2, CO, CO_2, NO, NO_2, H_2O_2, H_2O, NH_3, and hydrocarbons as disclosed by ReaxFF-MD simulations [190–197]. The size effects of the oxidation of ANPs are also investigated that under the same reaction condition, smaller ANPs become more explosive and form longer chain-like intermediates during the oxidation (Fig. 6f). Recently, Li *et al.* [198] further studied the oxidation of molten ANPs and proposed a microexplosion-accelerated oxidation mechanism as a supplement to our work. Jiang *et al.* [105] discovered that the addition of graphene oxide could enhance the combustion properties of ANPs in oxygen and improve their efficiency. By contrast, encapsulating ANPs into carbon nanotubes through self-assembly effectively suppresses the oxidation kinetics [199]. Surface oxides on Al nanoclusters were recently found to play an important role in exhibiting distinct optical properties such as photoluminescence [200].

Apart from aluminium, copper and copper oxide nanoparticles have also drawn great attention due to their excellent application value in many areas like gas sensors [201], microbiology [202] and catalysis [203]. Recently, the oxidation mechanism of copper nanoparticles has been investigated through ReaxFF-MD simulations [114]. The two most common configurations of copper oxide are the core/shell structure and hollow oxide structure. They can be explained by Cabrera-Mott theory and nanoscale Kirkendall effect, respectively. However, LaGrow et al. [183] found a different oxidation mechanism of copper nanoparticles. Fig. 6g shows the configuration of copper nanoparticles with a diameter of 3 nm after structure optimisation. Correspondingly, Fig. 6h shows the potential energy of the atoms. The atoms with less coordination number have the higher reactive potential energy. Oxygen tends to adsorb and dissociate at these highly reactive sites and form an initial oxidation structure. We use the notation of Cu^{i+}, which represent the different number of O atoms bonded to Cu atoms, to distinguish different oxides of Cu. The oxidation of copper nanoparticles is a process that oxides change from low coordination structure to high coordination structure. Finally, a core/shell oxide morphology forms, which consists of a thin oxide film and an unoxidised copper core. As the oxidation processes, the number of Cu^{1+} firstly increases and then decreases, transforming high coordination structure. Finally, the oxide shell is composed of Cu^{1+}, Cu^{2+} and Cu^{3+} structures. The influence of oxygen contents is also investigated. The simulation results showed in Fig. 6i suggested the increase of oxygen contents can only promote the oxidation degree to a limited extent, but had little effect on the transformation of oxides structure.

In summary, the complicated interplay between the structures of the oxidised nanoparticles with the reaction conditions suggests a promising avenue that take advantage of the oxidation process to fabricate various oxide nanostructures and metal/oxide nanocomposites, such as hollow nanostructures, metal/oxide core–shell nanoparticles, nanoporous oxides, ultra-thin dendritic oxide nanowires, and oxide clusters with tunable composition, architecture, defect structure, and properties. Modern computational approaches are able to reveal the oxidation mechanisms of nanoparticles and predict the generated oxide nanostructures in different environmental conditions, which could facilitate the design and fabrication of novel nanostructures for catalytic and electronic applications.

4.2. Oxidation of nanowires: Native oxides with unusual properties

Nanowires have attracted intensive attention because of their unique structures and properties serving as building blocks in various areas such as electronic nanodevices, electrocatalysis, and chemical sensing [204–210]. Many metallic or nonmetallic nanowires show superplasticity at room temperature, which could form single atomic chains under tension deformation and exhibit interesting electrical transport properties [209–211]. Also, the curved surfaces of nanowires and nanoparticles can provide abundant active sites in catalytic reactions. For example, Ultrafine jagged Pt nanowires were recently found to have extraordinary catalytic performance in the ORR due to the distinct active site distribution on the surface [61,206]. However, these curved surfaces, which are composed of undercoordinated atoms, could be vulnerable to oxygen-containing moieties (O_2, CO, H_2O, OH^-, etc.) and lead to deactivation in operating conditions [212,213]. Besides, the mechanical and electronic properties of nanowires are also strongly affected by surface oxidation. Therefore, understanding the interactions between the surface structures of nanowires with environmental species is of vital importance to improve their durability in operating conditions. Advanced atomistic simulation toolkits enable one to visualise how the surface atoms reorganise during the oxidation, as well as to probe the oxidation-induced variation in the properties of nanowires.

For a specific element, the oxidation kinetics of nanowires is thought to be faster than bulk surfaces and slower than nanoparticles with the same radius. This was theoretically evaluated by Zhdanov *et al.* [3,214] *via* extending the Cabrera-Mott model into the nanowire and nanoparticle systems. This discrepancy can also be understood at the atomic level. The ratio of active sites determines the initial reaction rate, while oxidation-induced lattice strain can promote the subsequent oxide growth, which is more significant in curved surfaces. Therefore, the oxidation rate follows the order: nanoparticle > nanowire > bulk.

The size dependence of the mechanical properties of nanowires was controversial. Many experimental and theoretical research investigated how the Young's modulus of nanowires changes with the diameter, while opposite conclusions were drawn because of neglecting the crucial effects of surface oxidation [215]. The environmental factors on the mechanical properties of materials become dominant when the size is reduced to the nanoscale. The extremely high surface-to-volume ratio of nanomaterials implies that a subtle change in the surface structure can result in tremendous variations in the overall properties. In recent years, van Duin and co-workers have conducted intensive computational work to investigate how surface oxidation affects the mechanical properties of nanowires based on the ReaxFF-MD simulation [216–222].

Sen *et al.* [217] performed computational studies and found the oxidation-induced softening of Al nanowires due to the peculiar structure of the surface oxide layer. First, ReaxFF-MD simulations unravelled that the native oxide shell has a relatively low density of 2.8 g/cm^3, compared with 4.0 g/cm^3 of bulk amorphous Al_2O_3. Static calculations showed that reducing the density of the amorphous Al_2O_3 from 4.0 g/cm^3 to 2.8 g/cm^3 can lead to a reduction in the Young's modulus from 103.21 to 81.36 GPa. More importantly, as shown in Fig. 7a, the stoichiometry of the native oxide shell formed on Al nanowires is $AlO_{1.1}$, rather than Al_2O_3, which is consistent with the conditions of surface oxides on ANPs [108]. The lower stoichiometry further decreases the Young's modulus to 57.50 GPa. Finally, the atomic coordination environment in the native oxide shell (Al atoms coordinate with 2.8 O atoms, and O atoms coordinate with 2.6 Al atoms in average) is quite different

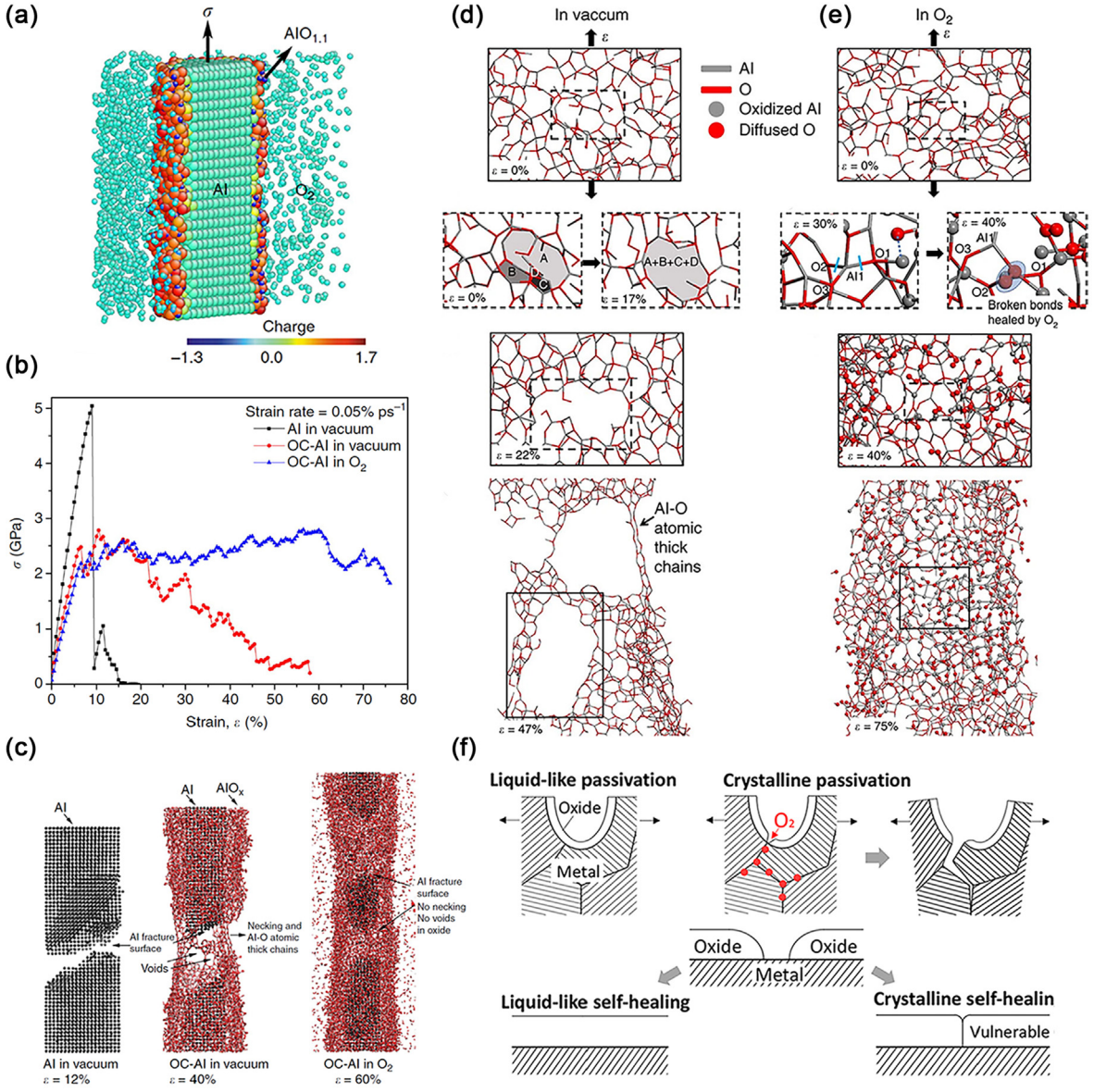

Fig. 7. Oxidation-enhanced ductility of Al nanowires. (a) Cross-section of the oxidised Al nanowire with atomic charge distribution. (b) A comparison of the computed stress–strain curves for the pure Al nanowire in vacuum, oxidised Al nanowire in vacuum, and oxidised Al nanowire in O_2. (c) Atomic structures of the Al nanowires during the deformation in the aforementioned three conditions. Atomic-scale deformation mechanism of the amorphous oxide layers in (d) vacuum and (e) O_2-rich environment. (f) A comparison of the passivation performance between crystalline and amorphous oxide layers [218,223].

from that in the oxides with the same stoichiometry obtained by the melt-quench method (Al atoms coordinate with 3.8 O atoms, and O atoms coordinate with 3.5 Al atoms in average). Due to the relatively low average Al-O coordinate numbers, the interatomic electrostatic forces are much weaker, which finally reduces the Young's modulus of the native oxide shell to 25.50 GPa. Such low Al-O coordinate environment in surface oxides formed by oxidation is also seen in the ANP system (Fig. 7b). In addition, simulations predicted that the Young's modulus of a nanowire is correlated with its diameter, following the rule of "smaller is softer".

The native oxide shell on Al nanowires formed by oxidation (E = 25.50 GPa) is much softer than pure Al nanowires (E ≈ 61 GPa), which is opposite to our conventional knowledge of the mechanical properties of metals and their oxides. Sen *et al.* [218] further explored how this oxide shell affects the mechanical properties of nanowires during tensile deformation. As shown in Fig. 7-b-c, three different model systems were utilised in the stretching simulations—a pure Al nanowire in vacuum, an oxidised Al nanowire in vacuum, and an oxidised Al nanowire in O_2. ReaxFF-MD simulations predicted the stress–strain curves of these samples with a constant strain rate of 0.05 % ps^{-1}. In vacuum, the Al nanowire has a high yield strength of 5 GPa and exhibits brittle fracture at ε = 12 % without necking, while the oxidised one forms a neck at ε = 12 % and fractures at ε = 40 %. It can be seen that the ductility of Al nanowires is enhanced by the surface oxides.

To probe into the atomistic origin of the oxidation-induced ductility enhancement of Al nanowires, they further studied the mechanism of defect formation during the deformation process. The determinant factor for the yielding stress and fracture limit is the nucleation of Shockley partial dislocations at the surface. The more movable dislocations there are in a material, the better ductility it has in the tensile deformation. Theoretical calculations showed that the Al/AlO_x interface could lower the activation energy for dis-

location nucleation, which could ease the yielding and facilitate the dislocation initiation. The Al/AlO_x interface also hinders the escape of dislocations from the surface and prolongs their duration. Therefore, the ductility of Al nanowires is improved by surface oxidation. How can the O_2-rich environment further enhance ductility? Fig. 7-d-e shows a comparison of the evolution of the Al-O bond networks in the oxide layers during the deformation in vacuum and O_2. Under vacuum, a significant feature in atomic-scale deformation is the formation of larger rings (with more than 14 atoms) at the expense of smaller rings, resulting in the growth of voids during the elongation of Al nanowires. These voids enlarge further and generate atomic chains before the fracture. By contrast, in the O_2-rich environment, an opposite Al-O ring evolution pattern occurs in which the number of larger rings gradually decreases with the increased smaller rings. This is because the environmental O_2 molecules chemisorb at the surface and "heals" the broken Al-O bonds, supplementing the voids and prohibiting their propagation.

Amorphous oxides are effective protective materials in industrial applications. The plasticity of the protective layers and its adherence to metal are the critical factors for preventing environmental degradation [223]. Passivation with crystalline oxides is vulnerable to stress-corrosion cracking, while amorphous oxides are less susceptible because of their better plasticity. As shown in Fig. 7f, if the crystalline oxide layer over the grain boundaries of the metal breaks up under stress, it cannot be repaired quickly so that detrimental molecules such as O_2, H_2O, S_8, and CO could easily diffuse inward along the grain boundary network [110,158,161]. This can substantially promote internal oxidation and result in intergranular crack propagation and material failure. Ideally, the cracks on the surface oxides could heal themselves like closing the wounds surgically, which can significantly protect the inner structures. This property is called "self-healing" [224,225], which requires a liquid-like superplasticity of the oxide layer.

4.3. Oxidation of two-dimensional nanosheets: defect-promotion and the formation of oxide chains

2D materials have unusual electronic, optical and mechanical properties, which have received extensive attention from both theoreticians and experimentalists in the past two decades [226–229]. Graphene [230,231], silicone [232], boron nitrides [233], and MXenes [234,235] are some examples of 2D materials that have been widely studied. Similar to other materials in nature, when preparing 2D materials and applying them in various fields, their oxidation stability is of great concern [236]. At the same time, the precise preparation of 2D oxides materials is as important as their corrosion protection. Direct synthesis of 2D metal oxides from liquid metals through oxidation is becoming one of the most promising approaches [8,17]. In response to the lack of a fundamental understanding of the oxidation processes of 2D materials, many researchers have studied this pivotal process both experimentally and theoretically. Specifically, atomic-scale modelling approaches enable one to investigate how the oxidation proceeds on the nanosheets and probe the possible products and the resulting nanostructures of the 2D oxides.

For example, the defect-promoted oxidation could be investigated at the atomic-scale by computer simulations. Pristine graphene has very low chemical activity, which is theoretically able to maintain its properties under extreme conditions. However, even a tiny imperfection could initiate graphene oxidation, and single vacancy defects [237,238], multiple vacancy defects [238], line defects, or grain boundaries [239] are in practical terms unavoidable during the preparation of graphene. Due to the different geometry structures and potential energy [240], different types of defects should change the topology and bonding structures of carbon atoms, which could further affect the chemical reactivity [241] and the oxidation mechanisms and kinetics. In fact, introducing a specific defect such as a single-atom vacancy and observing the atomic-scale oxidation processes at this site are hard to realise in real-time through experimental techniques, which computational approaches could alternatively provide valuable information.

Recently, based on ReaxFF-MD simulations, we explored the atomistic mechanism during the oxidation of graphene with or without defects [242]. By subtracting carbon atoms from the pristine sheet, single-vacancy defect (SVD) graphene and multi-vacancy defect (MVD) graphene were obtained [243]. We also created three models of graphene containing grain boundaries (GB 4–8, 5–8-5A1 and 5–8-5D) [244]. The nomenclature for GBs is based on the number of C atoms in the periodic disordered rings [240]. The normal coordination number of a C atom in pristine graphene is 3, but C atoms at a vacancy site will become under-coordination, making O_2 adsorption easier in energetics. The initial oxidation stage leads to an enlargement of the vacancy and the dissociation of carbon atoms, splitting the graphene sheet into two or more pieces. This reaction eventually leads to the destruction of the ordered hexagonal structure into disordered carbon oxide chains. Interestingly, during the oxidation of the SVD graphene, we found that the symmetry of the original vacancy site is preserved. As an example, five rounds of the escape of C atoms are shown in Fig. 8a. The GB structures show a tendency to self-restructure their disordered rings during oxidation. Each kind of GB consists of some disordered rings with 4–8 carbon atoms prior to oxidation. The rings containing more than 8 atoms would be identified as vacancies. Disordered rings are intrinsically unstable and prone to spontaneous rearrangement during any reaction. During the oxidation of GB graphenes, this tendency manifests as self-repairing and recombination of the disordered rings, as shown in Fig. 8b-d. These results suggest that in all cases, the oxidation proceeded along the GB, showing the inherent weakness of this type of defect towards oxidation. In addition, using *in situ* atomic force microscopy based on dynamic force mapping, Froning *et al.* mapped the chemical oxidation of an individual graphene flake during UV/ozone treatment against topography and clearly showed that oxidation begins at the edge of the graphene flake [245]. Lofti *et al.* heated the $Ti_3C_2O_2$ MXene at 1500 K in the presence of dry air and found that some defects were created on the MXene surface, and the size of these defects increased by time [107], shown in Fig. 8e. As a result, some O atoms diffuse to the MXene structure and facilitate the Ti atoms in the middle layer to diffuse to the surface and form TiO_2, demonstrating that defects could promote the oxidation of 2D materials. Rao *et al.* performed oxidation on few layer MoS_2 films while monitoring their Raman spectra *in situ* [246]. From analysis of the temperature-dependent decay rates and resonance Raman spectroscopy, they correlated oxidation rates to the ratio of structural defects in the MoS_2 films that defects are responsible for initiating and accelerating oxidation. These studies have both experimentally and theoretically demonstrated that the oxidation of 2D materials would generally start at the edge or defect sites of the sheets where the atoms are under-coordinated, serving as the active sites for the dissociative adsorption of oxygen molecules.

Apart from the common defect-promotion, the formation of oxide chains as oxidation products is commonly observed in the simulation of oxidation of 2D materials. Lotfi *et al.* [107] found that during the oxidation of $Ti_3C_2O_2$ Mxene, the two separate carbon layers went closer to each other, leading to the formation of C–C bonds and the carbon chains. In our work on the oxidation of MXenes with different layer numbers, we observe not only the formation of carbon chains, but also the eruption of the chains outside the MXenes sheet [95]. The morphological evolution of MXenes is shown in Fig. 9a-c. The oxidation of the MXene sheet begins with the adsorption of O atoms on the surface Ti layers. Then, the orig-

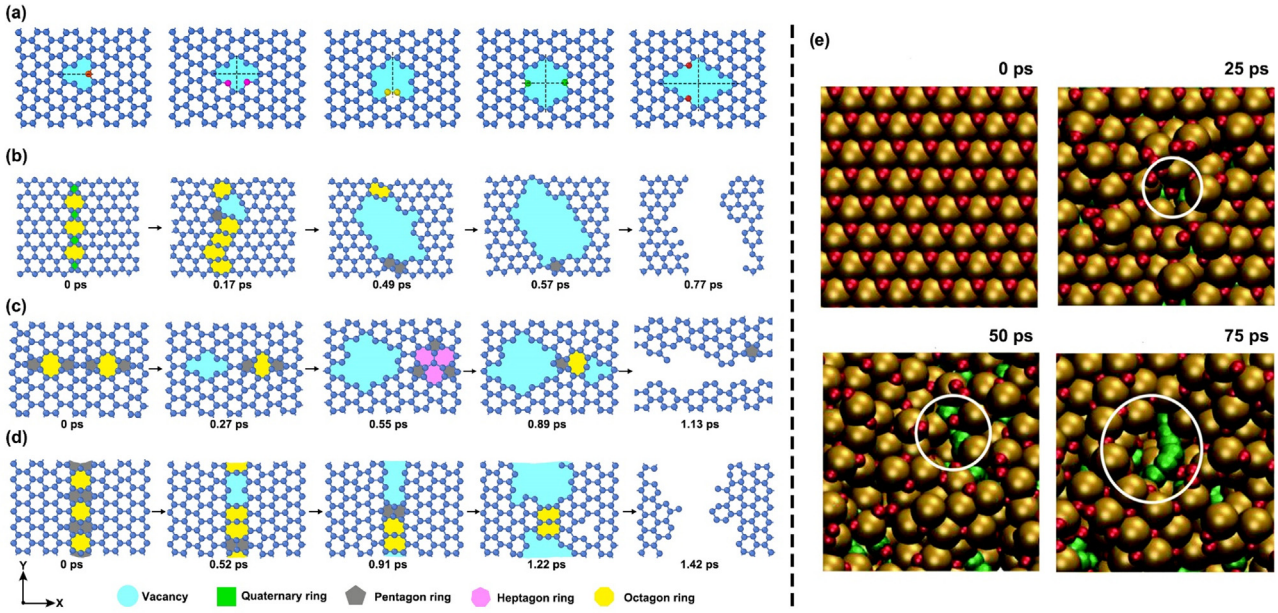

Fig. 8. Defect-promoted oxidation of 2D materials. (a) Symmetrical escape of C atoms on SVD graphene. The C atoms escaping in each round are depicted by different colours. Snapshots of structural evolutions of graphene with (b) 4–8 GB (c) 5–8-5A1 GB (d) 5–8-5D GB. Vacancies and disordered rings are indicated by different padding colours: cyan for vacancies, green for quaternary rings, grey for pentagon rings, pink for heptagon rings, and yellow for octagon rings. (e) Defect creation and enlargement during MXene heating at 1500 K in the presence of dry air (Ti: tan, C: green, O: red) [96,107]. (For interpretation of the references to colour in this figure legend, the reader is referred to the web version of this article.)

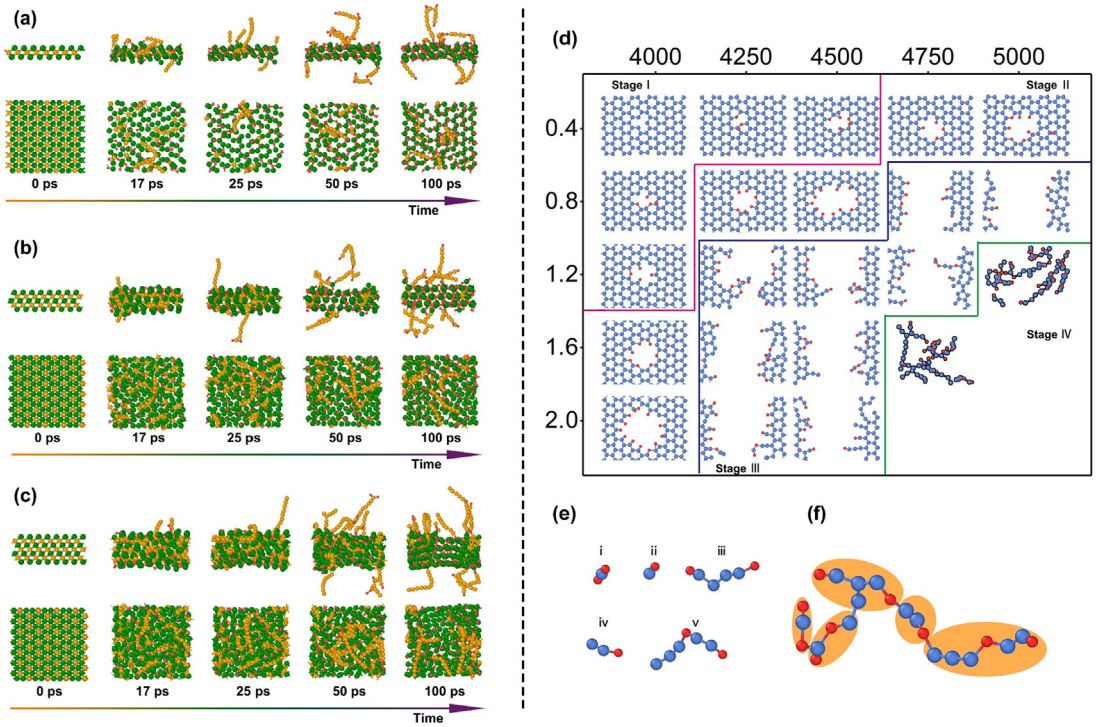

Fig. 9. The morphological evolution of (a) Ti_2C (b) Ti_3C_2 (c) Ti_4C_3 during the oxidation at 1000 K. (d) Structural phase diagram of the SVD graphene oxidation stage. (e) (f) Typical example of carbon oxide chains and their basic unit in stage IV. (i) CO_2 (ii) CO (iii) (iv) (v) Carbon oxide clusters [95,96].

inal lattice arrangement of Ti atoms start to distort, which induces the fracture of Ti-C bonds. Without the constraint from Ti atoms, free C atoms subsequently reassemble and form C—C bonds, generating some new carbon chains inside the sheet. Once the length of carbon chains gets too long to be trapped inside, the chains would erupt out of the sheets. Finally, a titanic oxide sheet with suspending carbon oxide chains and a few stuck C atoms are obtained. Increasing the layer number of the MXene could have a counteractive effect on the formation and eruption of carbon chains. Additionally, returning back to the graphene system, the sheet would crack apart eventually, and the ultimate oxidation product is carbon oxide chains at the final stage of oxidation, as shown in

Fig. 9d [242]. There are three basic units to combine the chains, such as CO, CO_2 and carbon oxide clusters, depicted in Fig. 9e, and these clusters were observed to either combine or separate to form or break chains due to the thermal motion. Fig. 9f shows a typical example of the carbon oxide chains.

In summary, by utilising modern computational methods, one could investigate the real-time oxidation of 2D materials at the atomic scale, calculate the accuracy energy diagram, and predict the oxidation products under various environmental conditions. Importantly, the thermodynamics of oxygen molecule adsorption and dissociation that play a pivotal role in the initial oxidation stage could be quantitatively calculated through first-principles-based approaches. Active sites can also be precisely identified at the atomic level of accuracy. By utilising MD simulations, we proved that defects in 2D materials are the common culprit for oxidation. We also observed the nucleation of the oxides at the defect sites and the formation of the oxide chains as oxidation products. We believe that computational methods have become a powerful instrument that opens up an attractive field for future studies of the oxidation stability of 2D materials and guides experimental fabrications.

5. Future challenges

In the future, with the rapid development of computer hardware and open-source codes, theoretical and computational approaches will continue to play an indispensable role in understanding oxidation, corrosion, catalysis, and other surface reactions. Despite the rapid development of computational approaches, there is still plenty of room for improving the computational approaches:

(1) Development of universal ReaxFFs with improved transferability and accuracy. At the current stage, existing ReaxFFs may not give reasonable accuracy beyond the trained reactions. The lack of transferability between the aqueous and combustion branches is also known, which could lead to problems in describing multi-phase interactions [56]. At present, genetic algorithms, deep learning, and machine learning (ML) techniques have already created new paradigms for force-field development, including high-throughput dataset generation through first-principles approaches and automatic ReaxFF parameterisation [60,169,170,172] one of the greatest challenges is developing universal ReaxFFs for a wide range of elements and complex reactions, which could greatly benefit the investigations of oxidation-resistance of complex materials such as high-entropy alloys [131] and multi-component metal nanoparticles [247]. Additionally, a particular interest could be centred on modelling the oxidation dynamics of liquids and liquid-oxide interfaces, which remains unclear in terms of the atomic-level mechanisms and is of great importance for synthesising high-quality 2D oxides [8,17,18]. Liquid-solid phase transition and multi-phase interactions should be considered simultaneously in the ReaxFF development in these studies.

(2) Accurate electronic-structure methods for modelling solid–gas interactions. The accuracy of DFT calculations highly relies on the approximation methods used. For example, a well-known debate exists on the dissociative adsorption of O_2 on the Al(1 1 1) surface [248]. While experiments provide solid evidence for a very low dissociative sticking probability of O_2 with a substantial energy barrier, standard DFT calculations found no barrier and provided little information on the atomistic origin. Based on modified high-level DFT calculations, various mechanisms have been proposed to explain this phenomenon, including spin selection rules [186], charge transfer [249], and steric effect [142,250]. Therefore, hybrid functionals [251] and high-level quantum chemistry methods [252] could be used to calculate the adsorption, migration, reaction energies, and vibrational frequencies for improved accuracy. Moreover, embedded-cluster approaches are powerful tools for obtaining accurate energetics of defect formation in oxides [253–256] and surface reactions [257–259], which avoid the spurious interactions between images in periodic boundary conditions.

(3) Combination of theoretical modelling with experimental studies. Despite massive research that has been conducted, many computational studies remained focusing on oxidation mechanisms while providing little guidance to the experimental design. We expect that much effort will be devoted to strengthening the link between theories and experiments to study oxidation in the near future. First, traditional electronic-structure methods and force-field based calculations should routinely be coupled with free energy calculations and thermodynamics to monitor environmental conditions [124]. Second, ReaxFF-MD and AIMD simulations should carefully consider the configurations of modelling systems to reveal the environmental effects on oxide properties and target atomistic details that are hard to be captured by microscopical observations [19,26,123]. Third, computational modelling has reached the high-throughput era in which a large amount of data can be automatically generated and analysed based on first-principles approaches. ML algorithms and data mining techniques could significantly assist the corrosion risk assessments and discoveries of novel anti-oxidation and corrosion protection materials [103,260–263]. DFT calculations will continue to play an essential role in providing reliable datasets and determining the descriptors for ML techniques.

6. Concluding remarks

In the past few decades, with the rapid development of computer hardware, QM theories, and modern algorithms, computer modelling provides the capacity to model, probe, and analyse physicochemical reactions in real-time at the atomic level. Based on mature theories and modern computational techniques, the mysteries in material oxidation are being gradually unveiled and systematically understood, enabling us to design practical anti-corrosion techniques and novel oxide-based functional materials.

The cross-fertilisation of various computational approaches provides an exciting avenue for unravelling novel oxidation mechanisms and guiding experimental synthesis. ReaxFF-MD and AIMD simulations allow us to visualise the dynamical evolutions of multiscale materials under reaction conditions. DFT calculations revealed that the adsorption energy, dissociation barrier of O_2, and diffusivity of ions are the key elements to determine the initial stage of oxidation. GCMC and *ab initio* thermodynamics play a vital role in predicting the stability of *meta*-stable oxides in realistic environments. ML techniques opened new doors for high-throughput experimental data analysis, materials design, and ReaxFF development.

Cabrera-Mott theory stands out as a widely accepted physical model that has been extended to various fields and inspired the synthesis of advanced materials such as 2D oxides and hollow nanostructures. Structural defects in materials play an essential role in enhancing the oxidation kinetics, which are the crucial factors of materials degradation and failure. Oxidation mechanisms of nanomaterials have recently attracted broad attention and can be delicately investigated by combining theoretical approaches with

experimental studies. Nanoparticles have enormously high proportions of active sites on the surface, resulting in diverse nanostructures such as core–shell structure, hollow nanoparticles, porous oxides, and chain-like oxides. Oxidation is usually detrimental to mechanical properties, while the native oxides formed on Al and Si nanowires on the contrary enhance their ductility due to the distinct amorphous structures. As for the 2D nanosheets, the oxidation kinetics is drastically accelerated by various structural defects, and oxide chains are commonly observed in the products.

The future will envision the integration of various computational techniques to develop reliable force fields, improve accuracy for describing solid–gas interactions, and model surface oxidation in realistic conditions. This integration will further combine with modern experimental techniques to complete the stories of oxidation theories, design next-generation oxidation-resistance strategies, and fabricate cutting-edge oxide materials with outstanding properties.

Declaration of Competing Interest

The authors declare that they have no known competing financial interests or personal relationships that could have appeared to influence the work reported in this paper.

Acknowledgements

The authors would like to acknowledge the support from the National Natural Science Foundation of China (Grant Nos. U1806219 and 52171038). This work is also supported by the Special Funding in the Project of the Taishan Scholar Construction Engineering and the program of Jinan Science and Technology Bureau (2020GXRC019) as well as new material demonstration platform construction project from Ministry of Industry and Information Technology (2020-370104-34-03-043952-01-11). Additionally, Xingfan Zhang thanks Han Yu for her fruitful discussions over the course of this work.

References

[1] N. Cabrera, N. Mott, Theory of the oxidation of metals, Rep. Prog. Phys. 12 (1) (1949) 163.
[2] S.K. Sankaranarayanan, E. Kaxiras, S. Ramanathan, Atomistic simulation of field enhanced oxidation of Al (100) beyond the Mott potential, Phys. Rev. Lett. 102 (9) (2009) 095504.
[3] V.P. Zhdanov, B. Kasemo, Cabrera-Mott kinetics of oxidation of nm-sized metal particles, Chem. Phys. Lett. 452 (4) (2008) 285–288.
[4] J.D. Baran, H. Grönbeck, A. Hellman, Mechanism for limiting thickness of thin oxide films on aluminum, Phys. Rev. Lett. 112 (14) (2014) 146103.
[5] R.S. Datta, N. Syed, A. Zavabeti, A. Jannat, M. Mohiuddin, M. Rokunuzzaman, B. Yue Zhang, M. Rahman, P. Atkin, K.A. Messalea, Flexible two-dimensional indium tin oxide fabricated using a liquid metal printing technique, Nat. Electron. 3 (1) (2020) 51–58.
[6] T. Alkathiri, N. Dhar, A. Jannat, N. Syed, M. Mohiuddin, M.M. Alsaif, R.S. Datta, K.A. Messalea, B.Y. Zhang, M.W. Khan, Atomically thin TiO 2 nanosheets synthesized using liquid metal chemistry, Chem. Commun. 56 (36) (2020) 4914–4917.
[7] J. Verjauw, A. Potočnik, M. Mongillo, R. Acharya, F. Mohiyaddin, G. Simion, A. Pacco, T. Ivanov, D. Wan, A. Vanleenhove, Investigation of microwave loss induced by oxide regrowth in high-Q niobium resonators, Phys. Rev. Appl. 16 (1) (2021) 014018.
[8] P. Aukarasereenont, A. Goff, C.K. Nguyen, C.F. McConville, A. Elbourne, A. Zavabeti, T. Daeneke, Liquid metals: an ideal platform for the synthesis of two-dimensional materials, Chem. Soc. Rev. (2022).
[9] L.P. Ramírez, F. Bournel, J.-J. Gallet, L. Dudy, F.o. Rochet, Testing the Cabrera–Mott oxidation model for aluminum under realistic conditions with near-ambient pressure photoemission, J. Phys. Chem. C (2022).
[10] X. Li, D. Zhang, Z. Liu, Z. Li, C. Du, C. Dong, Materials science: Share corrosion data, Nature 527 (7579) (2015) 441–442.
[11] B. Hou, X. Li, X. Ma, C. Du, D. Zhang, M. Zheng, W. Xu, D. Lu, F. Ma, The cost of corrosion in China, npj Mater, Degrad. 1 (1) (2017) 1–10.
[12] X. Li, S. Fu, W. Zhang, S. Ke, W. Song, J. Fang, Chemical anti-corrosion strategy for stable inverted perovskite solar cells, Sci. Adv. 6 (51) (2020) eabd1580.
[13] F. Shi, W. Gao, H. Shan, F. Li, Y. Xiong, J. Peng, Q. Xiang, W. Chen, P. Tao, C. Song, Strain-induced corrosion kinetics at nanoscale are revealed in liquid: enabling control of corrosion dynamics of electrocatalysis, Chem 6 (9) (2020) 2257–2271.
[14] T.J. Hersbach, M.T. Koper, Cathodic corrosion: 21st century insights into a 19th century phenomenon, Curr. Opin. Electrochem. 26 (2021) 100653.
[15] M. Bibes, J.E. Villegas, A. Barthelemy, Ultrathin oxide films and interfaces for electronics and spintronics, Adv. Phys. 60 (1) (2011) 5–84.
[16] M. Tsuchiya, S.K. Sankaranarayanan, S. Ramanathan, Photon-assisted oxidation and oxide thin film synthesis: A review, Prog. Mater. Sci. 54 (7) (2009) 981–1057.
[17] S. Zhao, J. Zhang, L. Fu, Liquid metals: a novel possibility of fabricating 2D metal oxides, Adv. Mater. 33 (9) (2021) 2005544.
[18] A. Zavabeti, J.Z. Ou, B.J. Carey, N. Syed, R. Orrell-Trigg, E.L. Mayes, C. Xu, O. Kavehei, A.P. O'Mullane, R.B. Kaner, A liquid metal reaction environment for the room-temperature synthesis of atomically thin metal oxides, Science 358 (6361) (2017) 332–335.
[19] Y. Sun, X. Zuo, S.K. Sankaranarayanan, S. Peng, B. Narayanan, G. Kamath, Quantitative 3D evolution of colloidal nanoparticle oxidation in solution, Science 356 (6335) (2017) 303–307.
[20] J. Feng, Y. Yin, Self-templating approaches to hollow nanostructures, Adv. Mater. 31 (38) (2019) 1802349.
[21] M. Fan, D. Liao, M.F.A. Aboud, I. Shakir, Y. Xu, A universal strategy toward ultrasmall hollow nanostructures with remarkable electrochemical performance, Angew. Chem. 132 (21) (2020) 8324–8331.
[22] W. Xia, Y. Yang, Q. Meng, Z. Deng, M. Gong, J. Wang, D. Wang, Y. Zhu, L. Sun, F. Xu, J. Li, H.L. Xin, Bimetallic nanoparticle oxidation in three dimensions by chemically sensitive electron tomography and in situ transmission electron microscopy, ACS Nano (2018).
[23] X. Sun, W. Zhu, D. Wu, Z. Liu, X. Chen, L. Yuan, G. Wang, R. Sharma, G. Zhou, Atomic-scale mechanism of unidirectional oxide growth, Adv. Funct. Mater. 30 (4) (2020) 1906504.
[24] D. Cadavid, A. Cabot, Oxidation at the atomic scale, Science 356(6335) (2017) 245-245.
[25] J. Peng, B. Chen, Z. Wang, J. Guo, B. Wu, S. Hao, Q. Zhang, L. Gu, Q. Zhou, Z. Liu, Surface coordination layer passivates oxidation of copper, Nature 586 (7829) (2020) 390–394.
[26] J. He, W.-H. Fang, R. Long, O.V. Prezhdo, Superoxide/peroxide chemistry extends charge carriers' lifetime but undermines chemical stability of CH3NH3PbI3 exposed to oxygen: time-domain ab initio analysis, J. Am. Chem. Soc. 141 (14) (2019) 5798–5807.
[27] B.Y. Zhang, K. Xu, Q. Yao, A. Jannat, G. Ren, M.R. Field, X. Wen, C. Zhou, A. Zavabeti, J.Z. Ou, Hexagonal metal oxide monolayers derived from the metal–gas interface, Nat. Mater. 20 (8) (2021) 1073–1078.
[28] R. Brenes, C. Eames, V. Bulović, M.S. Islam, S.D. Stranks, The impact of atmosphere on the local luminescence properties of metal halide perovskite grains, Adv. Mater. 30 (15) (2018) 1706208.
[29] N. Aristidou, C. Eames, I. Sanchez-Molina, X. Bu, J. Kosco, M.S. Islam, S.A. Haque, Fast oxygen diffusion and iodide defects mediate oxygen-induced degradation of perovskite solar cells, Nature Commun. 8 (1) (2017) 1–10.
[30] K. Chung, J. Bang, A. Thacharon, H.Y. Song, S.H. Kang, W.-S. Jang, N. Dhull, D. Thapa, C.M. Ajmal, B. Song, Non-oxidized bare copper nanoparticles with surface excess electrons in air, Nat. Nanotechnol. 1–7 (2022).
[31] W. Kohn, L.J. Sham, Self-consistent equations including exchange and correlation effects, Phys. Rev. 140 (4A) (1965) A1133.
[32] R.G. Parr, Density functional theory of atoms and molecules, Horizons of Quantum Chemistry, Springer, 1980, pp. 5–15.
[33] J.M. Haile, Molecular dynamics simulation: elementary methods, Wiley, New York, 1992.
[34] D. Adams, Grand canonical ensemble Monte Carlo for a Lennard-Jones fluid, Mol. Phys. 29 (1) (1975) 307–311.
[35] D. Marx, J. Hutter, Ab initio molecular dynamics: basic theory and advanced methods, Cambridge University Press, 2009.
[36] K. Reuter, C. Stampf, M. Scheffler, Ab initio atomistic thermodynamics and statistical mechanics of surface properties and functions, Handbook of materials modeling, Springer, 2005, pp. 149–194.
[37] P. Sherwood, A.H. de Vries, M.F. Guest, G. Schreckenbach, C.R.A. Catlow, S.A. French, A.A. Sokol, S.T. Bromley, W. Thiel, A.J. Turner, QUASI: A general purpose implementation of the QM/MM approach and its application to problems in catalysis, J. Mol. Struct.: THEOCHEM 632(1-3) (2003) 1-28.
[38] Y. Lum, T. Cheng, W.A. Goddard III, J.W. Ager, Electrochemical CO reduction builds solvent water into oxygenate products, J. Am. Chem. Soc. 140 (30) (2018) 9337–9340.
[39] Y.-Q. Su, J.-X. Liu, I.A. Filot, L. Zhang, E.J. Hensen, Highly active and stable CH4 oxidation by substitution of Ce4+ by two Pd2+ ions in CeO2 (111), ACS Catal. 8 (7) (2018) 6552–6559.
[40] C.E. Cash, J. Wang, M.M. Martirossyan, B.K. Ludlow, A.E. Baptista, N.M. Brown, E.J. Weissler, J. Abacousnac, S.J. Gerbode, Local melting attracts grain boundaries in colloidal polycrystals, Phys. Rev. Lett. 120 (1) (2018) 018002.
[41] T. Frenzel, M. Kadic, M. Wegener, Three-dimensional mechanical metamaterials with a twist, Science 358 (6366) (2017) 1072–1074.
[42] D. Tourret, Y. Song, A.J. Clarke, A. Karma, Grain growth competition during thin-sample directional solidification of dendritic microstructures: A phase-field study, Acta Mater. 122 (2017) 220–235.
[43] G. Henkelman, B.P. Uberuaga, H. Jónsson, A climbing image nudged elastic band method for finding saddle points and minimum energy paths, J. Chem. Phys. 113 (22) (2000) 9901–9904.

[44] K. Reuter, M. Scheffler, Composition, structure, and stability of RuO 2 (110) as a function of oxygen pressure, Phys. Rev. B 65 (3) (2001) 035406.
[45] W.A. Saidi, M. Lee, L. Li, G. Zhou, A.J. McGaughey, Ab initio atomistic thermodynamics study of the early stages of Cu (100) oxidation, Phys. Rev. B 86 (24) (2012) 245429.
[46] Q. Liu, L. Li, N. Cai, W.A. Saidi, G. Zhou, Oxygen chemisorption-induced surface phase transitions on Cu (110), Surf. Sci. 627 (2014) 75–84.
[47] Y. Shibuta, S. Sakane, E. Miyoshi, S. Okita, T. Takaki, M. Ohno, Heterogeneity in homogeneous nucleation from billion-atom molecular dynamics simulation of solidification of pure metal, Nature Commun. 8 (1) (2017) 1–9.
[48] M.R. Walsh, C.A. Koh, E.D. Sloan, A.K. Sum, D.T. Wu, Microsecond simulations of spontaneous methane hydrate nucleation and growth, Science 326 (5956) (2009) 1095–1098.
[49] A.J. O'Malley, V.G. Sakai, I.P. Silverwood, N. Dimitratos, S.F. Parker, C.R.A. Catlow, Methanol diffusion in zeolite HY: a combined quasielastic neutron scattering and molecular dynamics simulation study, Phys. Chem. Chem. Phys. 18 (26) (2016) 17294–17302.
[50] C. Sun, R. Zhou, B. Bai, Electrostatic Effect-based Selective Permeation Characteristics of Graphene Nanopores, Acta Phys.-Chim. Sin. 36 (11) (2020) 1911044.
[51] W. Wu, L. Zhang, S. Liu, H. Ren, X. Zhou, H. Li, Liquid–liquid phase transition in nanoconfined silicon carbide, J. Am. Chem. Soc. 138 (8) (2016) 2815–2822.
[52] T. Li, L. Zhang, X. Zhang, H. Li, Effect of curved surfaces on the impacting nano-droplets and their shape control: a molecular dynamics simulation study, Appl. Surf. Sci. 454 (2018) 192–200.
[53] E. Mosconi, F. De Angelis, Mobile ions in organohalide perovskites: interplay of electronic structure and dynamics, ACS Energy Lett. 1 (1) (2016) 182–188.
[54] A.K. Rappe, W.A. Goddard III, Charge equilibration for molecular dynamics simulations, J. Phys. Chem. 95 (8) (1991) 3358–3363.
[55] A.C. Van Duin, S. Dasgupta, F. Lorant, W.A. Goddard, ReaxFF: a reactive force field for hydrocarbons, J. Phys. Chem. A 105 (41) (2001) 9396–9409.
[56] T.P. Senftle, S. Hong, M.M. Islam, S.B. Kylasa, Y. Zheng, Y.K. Shin, C. Junkermeier, R. Engel-Herbert, M.J. Janik, H.M. Aktulga, The ReaxFF reactive force-field: development, applications and future directions, npj Comput, Mater. 2 (2016) 15011.
[57] A. Shekhar, K.-I. Nomura, R.K. Kalia, A. Nakano, P. Vashishta, Nanobubble collapse on a silica surface in water: Billion-atom reactive molecular dynamics simulations, Phys. Rev. Lett. 111 (18) (2013) 184503.
[58] J. Behler, Perspective: Machine learning potentials for atomistic simulations, J. Chem. Phys. 145 (17) (2016) 170901.
[59] D. Mora-Fonz, J.C. Schön, J. Prehl, S.M. Woodley, C.R.A. Catlow, A. Shluger, A.A. Sokol, Real and Virtual Polymorphism of Titanium Selenide with Robust Interatomic Potentials, J. Mater. Chem. A (2020).
[60] M.Y. Sengul, Y. Song, N. Nayir, Y. Gao, Y. Hung, T. Dasgupta, A.C. van Duin, INDEEDopt: a deep learning-based ReaxFF parameterization framework, npj Comput, Mater. 7 (1) (2021) 1–9.
[61] Y. Chen, T. Cheng, W.A. Goddard Iii, Atomistic Explanation of the Dramatically Improved Oxygen Reduction Reaction of Jagged Platinum Nanowires, 50 Times Better than Pt, J. Am. Chem. Soc. 142 (19) (2020) 8625–8632.
[62] L. Shi, Z. Ying, A. Xu, Y. Cheng, Unraveling the Water-Mediated Proton Conduction Mechanism along the Surface of Graphene Oxide, Chem. Mater. 32 (14) (2020) 6062–6069.
[63] Y. Liu, Z. Duan, J. Li, C. Chang, Gas-Phase Mechanism Study of Methane Nonoxidative Conversion by ReaxFF Method, Acta Phys.-Chim. Sin. 37 (11) (2021) 2011012.
[64] Q. Zhu, W.A. Saidi, J.C. Yang, Step-edge directed metal oxidation, J. Phys. Chem. Lett. 7 (13) (2016) 2530–2536.
[65] Q. Zhu, W.A. Saidi, J.C. Yang, Enhanced mass transfer in the step edge induced oxidation on Cu (100) surface, J. Phys. Chem. C 121 (21) (2017) 11251–11260.
[66] Q. Zhu, L. Zou, G. Zhou, W.A. Saidi, J.C. Yang, Early and transient stages of Cu oxidation: atomistic insights from theoretical simulations and in situ experiments, Surf. Sci. 652 (2016) 98–113.
[67] Q. Zhu, W.A. Saidi, J.C. Yang, Step-induced oxygen upward diffusion on stepped Cu (100) surface, J. Phys. Chem. C 119 (1) (2015) 251–261.
[68] K. Chenoweth, A.C. Van Duin, W.A. Goddard, ReaxFF reactive force field for molecular dynamics simulations of hydrocarbon oxidation, J. Phys. Chem. A 112 (5) (2008) 1040–1053.
[69] A.C. Van Duin, A. Strachan, S. Stewman, Q. Zhang, X. Xu, W.A. Goddard, ReaxFFSiO reactive force field for silicon and silicon oxide systems, J. Phys. Chem. A 107 (19) (2003) 3803–3811.
[70] N. Nayir, A.C.T. van Duin, S. Erkoc, Development of the ReaxFF Reactive Force Field for Inherent Point Defects in the Si/Silica System, J. Phys. Chem. A 123 (19) (2019) 4303–4313.
[71] D.A. Newsome, D. Sengupta, H. Foroutan, M.F. Russo, A.C.T. van Duin, Oxidation of Silicon Carbide by O_2 and H_2O: A ReaxFF Reactive Molecular Dynamics Study, Part I, J. Phys. Chem. C 116 (30) (2012) 16111–16121.
[72] A.D. Kulkarni, D.G. Truhlar, S. Goverapet Srinivasan, A.C. Van Duin, P. Norman, T.E. Schwartzentruber, Oxygen interactions with silica surfaces: Coupled cluster and density functional investigation and the development of a new ReaxFF potential, J. Phys. Chem. C 117 (1) (2013) 258–269.
[73] Y. Wang, Y. Shi, Q. Sun, K. Lu, M. Kubo, J. Xu, Development of a Transferable ReaxFF Parameter Set for Carbon-and Silicon-Based Solid Systems, J. Phys. Chem. C 124 (18) (2020) 10007–10015.
[74] T.P. Senftle, R.J. Meyer, M.J. Janik, A.C. van Duin, Development of a ReaxFF potential for Pd/O and application to palladium oxide formation, J. Chem. Phys. 139 (4) (2013) 044109.
[75] D. Fantauzzi, J. Bandlow, L. Sabo, J.E. Mueller, A.C. van Duin, T. Jacob, Development of a ReaxFF potential for Pt–O systems describing the energetics and dynamics of Pt-oxide formation, Phys. Chem. Chem. Phys. 16 (42) (2014) 23118–23133.
[76] D. Fantauzzi, J.E. Mueller, L. Sabo, A.C. Van Duin, T. Jacob, Surface buckling and subsurface oxygen: atomistic insights into the surface oxidation of Pt (111), ChemPhysChem 16 (13) (2015) 2797–2802.
[77] C. Zou, Y.K. Shin, A.C. van Duin, H. Fang, Z.-K. Liu, Molecular dynamics simulations of the effects of vacancies on nickel self-diffusion, oxygen diffusion and oxidation initiation in nickel, using the ReaxFF reactive force field, Acta Mater. 83 (2015) 102–112.
[78] Y.K. Shin, H. Kwak, A.V. Vasenkov, D. Sengupta, A.C.T. van Duin, Development of a ReaxFF Reactive Force Field for Fe/Cr/O/S and Application to Oxidation of Butane over a Pyrite-Covered Cr2O3 Catalyst, ACS Catal. 5 (12) (2015) 7226–7236.
[79] S. Hong, A.C.T. van Duin, Molecular Dynamics Simulations of the Oxidation of Aluminum Nanoparticles using the ReaxFF Reactive Force Field, J. Phys. Chem. C 119 (31) (2015) 17876–17886.
[80] S. Hong, A.C.T. van Duin, Atomistic-Scale Analysis of Carbon Coating and Its Effect on the Oxidation of Aluminum Nanoparticles by ReaxFF-Molecular Dynamics Simulations, J. Phys. Chem. C 120 (17) (2016) 9464–9474.
[81] Y. Zheng, S. Hong, G. Psofogiannakis, G.B. Rayner Jr, S. Datta, A.C. van Duin, R. Engel-Herbert, Modeling and in situ probing of surface reactions in atomic layer deposition, ACS Appl. Mater. Interfaces 9 (18) (2017) 15848–15856.
[82] N. Nayir, A.C. Van Duin, S. Erkoc, Development of a ReaxFF Reactive Force Field for Interstitial Oxygen in Germanium and Its Application to GeO2/Ge Interfaces, J. Phys. Chem. C 123 (2) (2018) 1208–1218.
[83] M. Aryanpour, A.C. van Duin, J.D. Kubicki, Development of a reactive force field for iron– oxyhydroxide systems, J. Phys. Chem. A 114 (21) (2010) 6298–6307.
[84] A. Lloyd, D. Cornil, A. Van Duin, D. van Duin, R. Smith, S. Kenny, J. Cornil, D. Beljonne, Development of a ReaxFF potential for Ag/Zn/O and application to Ag deposition on ZnO, Surf. Sci. 645 (2016) 67–73.
[85] K. Joshi, A.C. van Duin, T. Jacob, Development of a ReaxFF description of gold oxides and initial application to cold welding of partially oxidized gold surfaces, J. Mater. Chem. 20 (46) (2010) 10431–10437.
[86] M.H. Rahman, E.H. Chowdhury, S. Hong, High temperature oxidation of monolayer MoS2 and its effect on mechanical properties: A ReaxFF molecular dynamics study, Surf. Interfaces 26 (2021) 101371.
[87] N.C. Osti, M. Naguib, A. Ostadhossein, Y. Xie, P.R. Kent, B. Dyatkin, G. Rother, W.T. Heller, A.C. Van Duin, Y. Gogotsi, Effect of metal ion intercalation on the structure of MXene and water dynamics on its internal surfaces, ACS Appl. Mater. Interfaces 8 (14) (2016) 8859–8863.
[88] H.M. Aktulga, J.C. Fogarty, S.A. Pandit, A.Y. Grama, Parallel reactive molecular dynamics: Numerical methods and algorithmic techniques, Parallel Comput. 38 (4) (2012) 245–259.
[89] K. Chenoweth, A.C. van Duin, W.A. Goddard III, The ReaxFF Monte Carlo reactive dynamics method for predicting atomistic structures of disordered ceramics: application to the Mo3VOx Catalyst, Angew. Chem., Int. Ed. 48 (41) (2009) 7630–7634.
[90] T.P. Senftle, A.C. van Duin, M.J. Janik, Methane activation at the Pd/CeO2 interface, ACS Catal. 7 (1) (2017) 327–332.
[91] B. Kirchhoff, L. Braunwarth, C. Jung, H. Jónsson, D. Fantauzzi, T. Jacob, Simulations of the Oxidation and Degradation of Platinum Electrocatalysts, Small 16 (5) (2020) 1905159.
[92] D. Fantauzzi, S. Krick Calderón, J.E. Mueller, M. Grabau, C. Papp, H.P. Steinrück, T.P. Senftle, A.C. van Duin, T. Jacob, Growth of Stable Surface Oxides on Pt (111) at Near-Ambient Pressures, Angew. Chem., Int. Ed. 56 (10) (2017) 2594–2598.
[93] X. Zhang, Y. Duan, X. Dai, T. Li, Y. Xia, P. Zheng, H. Li, Y. Jiang, Atomistic origin of amorphous-structure-promoted oxidation of silicon, Appl. Surf. Sci. 504 (2020) 144437.
[94] J. Wen, T. Ma, W. Zhang, A.C. Van Duin, D.M. Van Duin, Y. Hu, X. Lu, Atomistic insights into Cu chemical mechanical polishing mechanism in aqueous hydrogen peroxide and glycine: ReaxFF reactive molecular dynamics simulations, J. Phys. Chem. C 123 (43) (2019) 26467–26474.
[95] P. Zheng, X. Zhang, M. Yan, Y. Ma, Y. Jiang, H. Li, The Eruption of Carbon Chains in the Oxidation of 2D Tin+ 1Cn (n= 1, 2, 3) MXenes, Appl. Surf. Sci. (2021) 149310.
[96] P. Zheng, X. Zhang, Y. Duan, M. Yan, R. Chapman, Y. Jiang, H. Li, Oxidation of graphene with variable defects: alternately symmetrical escape and self-restructuring of carbon rings, Nanoscale (2020).
[97] B. Devine, T.-R. Shan, Y.-T. Cheng, A.J. McGaughey, M. Lee, S.R. Phillpot, S.B. Sinnott, Atomistic simulations of copper oxidation and Cu/Cu 2 O interfaces using charge-optimized many-body potentials, Phys. Rev. B 84 (12) (2011) 125308.
[98] T.-R. Shan, B.D. Devine, T.W. Kemper, S.B. Sinnott, S.R. Phillpot, Charge-optimized many-body potential for the hafnium/hafnium oxide system, Phys. Rev. B 81 (12) (2010) 125328.
[99] Y.-T. Cheng, T.-R. Shan, T. Liang, R.K. Behera, S.R. Phillpot, S.B. Sinnott, A charge optimized many-body (comb) potential for titanium and titania, J. Phys.: Condensed Matter 26 (31) (2014) 315007.
[100] K. Ohno, K. Esfarjani, Y. Kawazoe, Computational materials science: from ab initio to Monte Carlo methods, Springer, 2018.
[101] I. Steinbach, Phase-field models in materials science, Modell. Simul. Mater. Sci. Eng. 17 (7) (2009) 073001.

[102] F. Roters, P. Eisenlohr, L. Hantcherli, D.D. Tjahjanto, T.R. Bieler, D. Raabe, Overview of constitutive laws, kinematics, homogenization and multiscale methods in crystal plasticity finite-element modeling: Theory, experiments, applications, Acta Mater. 58 (4) (2010) 1152–1211.
[103] K.T. Butler, D.W. Davies, H. Cartwright, O. Isayev, A. Walsh, Machine learning for molecular and materials science, Nature 559 (7715) (2018) 547–555.
[104] U. Khalilov, A. Bogaerts, E.C. Neyts, Toward the understanding of selective Si nano-oxidation by atomic scale simulations, Acc. Chem. Res. 50 (4) (2017) 796–804.
[105] Y. Jiang, S. Deng, S. Hong, J. Zhao, S. Huang, C.-C. Wu, J.L. Gottfried, K.-I. Nomura, Y. Li, S. Tiwari, R.K. Kalia, P. Vashishta, A. Nakano, X. Zheng, Energetic Performance of Optically Activated Aluminum/Graphene Oxide Composites, ACS Nano 12 (11) (2018) 11366–11375.
[106] J. Liu, Q. Wang, Y. Qi, Atomistic simulation of the formation and fracture of oxide bifilms in cast aluminum, Acta Mater. 164 (2019) 673–682.
[107] R. Lotfi, M. Naguib, D.E. Yilmaz, J. Nanda, A.C. Van Duin, A comparative study on the oxidation of two-dimensional Ti 3 C 2 MXene structures in different environments, J. Mater. Chem. A 6 (26) (2018) 12733–12743.
[108] X. Zhang, C. Fu, Y. Xia, Y. Duan, Y. Li, Z. Wang, Y. Jiang, H. Li, Atomistic Origin of the Complex Morphological Evolution of Aluminum Nanoparticles during Oxidation: A Chain-like Oxide Nucleation and Growth Mechanism, ACS Nano 13 (3) (2019) 3005–3014.
[109] P.-J. Yang, Q.-J. Li, T. Tsuru, S. Ogata, J.-W. Zhang, H.-W. Sheng, Z.-W. Shan, G. Sha, W.-Z. Han, J. Li, Mechanism of hardening and damage initiation in oxygen embrittlement of body-centred-cubic niobium, Acta Mater. 168 (2019) 331–342.
[110] G. Saleh, C. Xu, S. Sanvito, Silver Tarnishing Mechanism Revealed by Molecular Dynamics Simulations, Angew. Chem., Int. Ed. 58 (18) (2019) 6017–6021.
[111] K. Sasikumar, B. Narayanan, M. Cherukara, A. Kinaci, F.G. Sen, S.K. Gray, M.K. Chan, S.K. Sankaranarayanan, Evolutionary Optimization of a Charge Transfer Ionic Potential Model for Ta/Ta-Oxide Heterointerfaces, Chem. Mater. 29 (8) (2017) 3603–3614.
[112] K. Sasikumar, H. Chan, B. Narayanan, S.K.R.S. Sankaranarayanan, Machine Learning Applied to a Variable Charge Atomistic Model for Cu/Hf Binary Alloy Oxide Heterostructures, Chem. Mater. 31 (9) (2019) 3089–3102.
[113] S.S. Jo, A. Singh, L. Yang, S.C. Tiwari, S. Hong, A. Krishnamoorthy, M.G. Sales, S. M. Oliver, J. Fox, R.L. Cavalero, Growth Kinetics and Atomistic Mechanisms of Native Oxidation of ZrS x Se2–x and MoS2 Crystals, Nano Lett. 20 (12) (2020) 8592–8599.
[114] Y. Ma, X. Zhang, P. Zheng, E. Ni, Y. Wang, Y. Jiang, H. Li, Structural Transformation from Low-Coordinated Oxides to High-Coordinated Oxides during the Oxidation of Cu Nanoparticles, J. Phys. Chem. C 125 (16) (2021) 8759–8766.
[115] A.B. Puthirath, E.F. Oliveira, G. Gao, N. Chakingal, H. Kannan, C. Li, X. Zhang, A. Biswas, M.R. Neupane, B.B. Pate, Oxygenation of Diamond Surfaces via Hummer's Method, Chem. Mater. 33 (13) (2021) 4977–4987.
[116] D. Kumar, V. Jain, B. Rai, Capturing the synergistic effects between corrosion inhibitor molecules using density functional theory and ReaxFF simulations-A case for benzyl azide and butyn-1-ol on Cu surface, Corros. Sci. 195 (2022) 109960.
[117] L. Shi, M. Sessim, M.R. Tonks, S.R. Phillpot, High-temperature oxidation of carbon fiber and char by molecular dynamics simulation, Carbon 185 (2021) 449–463.
[118] R.B. Wexler, T. Qiu, A.M. Rappe, Automatic prediction of surface phase diagrams using ab initio grand canonical monte carlo, J. Phys. Chem. C 123 (4) (2019) 2321–2328.
[119] W.-Y. Lin, R. Huang, L. Li, Y.-H. Wen, Oxygen adsorption on high-index faceted Pt nanoparticles, Phys. Chem. Chem. Phys. 23 (32) (2021) 17323–17328.
[120] D. Mora-Fonz, T. Lazauskas, M.R. Farrow, C.R.A. Catlow, S.M. Woodley, A.A. Sokol, Why are polar surfaces of ZnO stable?, Chem Mater. 29 (12) (2017) 5306–5320.
[121] J. Pal, T.B. Rawal, M. Smerieri, S. Hong, M. Alatalo, L. Savio, L. Vattuone, T.S. Rahman, M. Rocca, Adatom Extraction from pristine metal terraces by dissociative oxygen adsorption: Combined STM and density functional theory investigation of O/Ag (110), Phys. Rev. Lett. 118 (22) (2017) 226101.
[122] Z. Fang, E. Wang, Y. Chen, X. Hou, K.-C. Chou, W. Yang, J. Chen, M. Shang, Wurtzite AlN (0001) surface oxidation: hints from ab initio calculations, ACS Appl. Mater. Interfaces 10 (36) (2018) 30811–30818.
[123] L. Luo, M. Su, P. Yan, L. Zou, D.K. Schreiber, D.R. Baer, Z. Zhu, G. Zhou, Y. Wang, S.M. Bruemmer, Atomic origins of water-vapour-promoted alloy oxidation, Nat. Mater. 17 (6) (2018) 514.
[124] S. Surendralal, M. Todorova, M.W. Finnis, J. Neugebauer, First-principles approach to model electrochemical reactions: understanding the fundamental mechanisms behind Mg corrosion, Phys. Rev. Lett. 120 (24) (2018) 246801.
[125] J. Ren, Y. Wang, J. Zhao, S. Tan, H. Petek, K atom promotion of O2 chemisorption on Au (111) surface, J. Am. Chem. Soc. 141 (10) (2019) 4438–4444.
[126] Q. Zhu, Z. Pan, Z. Zhao, G. Cao, L. Luo, C. Ni, H. Wei, Z. Zhang, F. Sansoz, J. Wang, Defect-driven selective metal oxidation at atomic scale, Nature Commun. 12 (1) (2021) 1–8.
[127] R. Maji, E. Luppi, N. Capron, E. Degoli, Ab initio study of oxygen segregation in silicon grain boundaries: The role of strain and vacancies, Acta Mater. 204 (2021) 116477.
[128] M. Li, M.T. Curnan, M.A. Gresh-Sill, S.D. House, W.A. Saidi, J.C. Yang, Unusual layer-by-layer growth of epitaxial oxide islands during Cu oxidation, Nature Commun. 12 (1) (2021) 1–7.
[129] V.J. Bukas, K. Reuter, Hot adatom diffusion following oxygen dissociation on Pd (100) and Pd (111): A first-principles study of the equilibration dynamics of exothermic surface reactions, Phys. Rev. Lett. 117 (14) (2016) 146101.
[130] M. Aykol, K.A. Persson, Oxidation protection with amorphous surface oxides: Thermodynamic insights from ab initio simulations on aluminum, ACS Appl. Mater. Interfaces 10 (3) (2018) 3039–3045.
[131] B. Song, Y. Yang, M. Rabbani, T.T. Yang, K. He, X. Hu, Y. Yuan, P. Ghildiyal, V.P. Dravid, M.R. Zachariah, In situ oxidation studies of high-entropy alloy nanoparticles, ACS nano 14 (11) (2020) 15131–15143.
[132] H. Guo, P. Poths, P. Sautet, A.N. Alexandrova, Oxidation Dynamics of Supported Catalytic Cu Clusters: Coupling to Fluxionality, ACS Catal. 12 (2021) 818–827.
[133] M. Capdevila-Cortada, N. López, Entropic contributions enhance polarity compensation for CeO 2 (100) surfaces, Nat. Mater. 16 (3) (2017) 328–334.
[134] A. Jonayat, S. Chen, A.C. Van Duin, M. Janik, Predicting Monolayer Oxide Stability over Low-Index Surfaces of TiO2 Polymorphs Using ab Initio Thermodynamics, Langmuir 34 (39) (2018) 11685–11694.
[135] K. Klyukin, A. Zagalskaya, V. Alexandrov, Ab initio thermodynamics of iridium surface oxidation and oxygen evolution reaction, J. Phys. Chem. C 122 (51) (2018) 29350–29358.
[136] Y.-J. Lee, T. Lee, A. Soon, Phase stability diagrams of group 6 Magnéli oxides and their implications for photon-assisted applications, Chem. Mater. 31 (11) (2019) 4282–4290.
[137] S. Hanselman, I.T. McCrum, M.J. Rost, M.T. Koper, Thermodynamics of the formation of surface PtO 2 stripes on Pt (111) in the absence of subsurface oxygen, Phys. Chem. Chem. Phys. 22 (19) (2020) 10634–10640.
[138] L.N. Walters, L.-F. Huang, J.M. Rondinelli, First-Principles-Based Prediction of Electrochemical Oxidation and Corrosion of Copper under Multiple Environmental Factors, J. Phys. Chem. C 125 (25) (2021) 14027–14038.
[139] Y.-J. Lee, T.T. Ly, T. Lee, K. Palotás, S.Y. Jeong, J. Kim, A. Soon, Completing the picture of initial oxidation on copper, Appl. Surf. Sci. 562 (2021) 150148.
[140] A. Jonayat, A.C. Van Duin, M.J. Janik, Discovery of descriptors for stable monolayer oxide coatings through machine learning, ACS Appl. Energy Mater. 1 (11) (2018) 6217–6226.
[141] G. Sun, A.N. Alexandrova, P. Sautet, Structural rearrangements of subnanometer Cu oxide clusters govern catalytic oxidation, ACS Catal. 10 (9) (2020) 5309–5317.
[142] R. Yin, Y. Zhang, F. Libisch, E.A. Carter, H. Guo, B. Jiang, Dissociative chemisorption of O2 on Al (111): dynamics on a correlated wave-function-based potential energy surface, J. Phys. Chem. Lett. 9 (12) (2018) 3271–3277.
[143] K.R. Lawless, The oxidation of metals, Rep. Prog. Phys. 37 (2) (1974) 231.
[144] A. Atkinson, Transport processes during the growth of oxide films at elevated temperature, Rev. Mod. Phys. 57 (2) (1985) 437.
[145] B. Hammer, J.K. Norskov, Why gold is the noblest of all the metals, Nature 376 (6537) (1995) 238–240.
[146] B. Hammer, J.K. Nørskov, Theoretical surface science and catalysis—calculations and concepts, Adv. Catal., Academic Press (2000) 71–129.
[147] J.K. Nørskov, F. Studt, F. Abild-Pedersen, T. Bligaard, Fundamental concepts in heterogeneous catalysis, John Wiley & Sons, 2014.
[148] H. Xin, A. Vojvodic, J. Voss, J.K. Nørskov, F. Abild-Pedersen, Effects of d-band shape on the surface reactivity of transition-metal alloys, Phys. Rev. B 89 (11) (2014) 115114.
[149] A.J. Samin, C.D. Taylor, A first principles investigation of the oxygen adsorption on Zr (0001) surface using cluster expansions, Appl. Surf. Sci. 423 (2017) 1035–1044.
[150] T.A. Baker, C.M. Friend, E. Kaxiras, Atomic oxygen adsorption on Au (111) surfaces with defects, J. Phys. Chem. C 113 (8) (2009) 3232–3238.
[151] F.P. Fehlner, N.F. Mott, Low-temperature oxidation, Oxidation of Metals 2 (1) (1970) 59–99.
[152] L. Hui, Influence of intermediate-range order on glass formation, J. Phys. Chem. B 108 (17) (2004) 5438–5442.
[153] D.B. Buchholz, Q. Ma, D. Alducin, A. Ponce, M. Jose-Yacaman, R. Khanal, J.E. Medvedeva, R.P. Chang, The structure and properties of amorphous indium oxide, Chem. Mater. 26 (18) (2014) 5401–5411.
[154] Y. Duan, J. Li, X. Zhang, T. Li, H. Arandiyan, Y. Jiang, H. Li, Crystallization behavior of a confined CuZr metallic liquid film with a sandwich-like structure, Phys. Chem. Chem. Phys. 21 (25) (2019) 13738–13745.
[155] L. Jeurgens, W. Sloof, F. Tichelaar, E. Mittemeijer, Thermodynamic stability of amorphous oxide films on metals: Application to aluminum oxide films on aluminum substrates, Phys. Rev. B 62 (7) (2000) 4707.
[156] L. Jeurgens, W. Sloof, F. Tichelaar, E. Mittemeijer, Growth kinetics and mechanisms of aluminum-oxide films formed by thermal oxidation of aluminum, J. Appl. Phys. 92 (3) (2002) 1649–1656.
[157] F. Reichel, L. Jeurgens, E. Mittemeijer, The thermodynamic stability of amorphous oxide overgrowths on metals, Acta Mater. 56 (3) (2008) 659–674.
[158] E.T. Bentria, G.K. N'tsouaglo, C.S. Becquart, O. Bouhali, N. Mousseau, F. El-Mellouhi, The role of emerging grain boundary at iron surface, temperature and hydrogen on metal dusting initiation, Acta Mater. 135 (2017) 340-347.
[159] L. Li, L. Luo, J. Ciston, W.A. Saidi, E.A. Stach, J.C. Yang, G. Zhou, Surface-step-induced oscillatory oxide growth, Phys. Rev. Lett. 113 (13) (2014) 136104.
[160] Y. Sun, Y.-L. Liu, S. Izumi, X.-F. Chen, Z. Zhai, S.-H. Tian, Initial stage oxidation on nano-trenched Si (1 0 0) surface, J. Phys. D: Appl. Phys. 51 (1) (2017) 015305.

[161] S.-I. Yamaura, S. Tsurekawa, T. Watanabe, The control of oxidation-induced intergranular embrittlement by grain boundary engineering in rapidly solidified Ni-Fe alloy ribbons, Mater. Trans. 44 (7) (2003) 1494–1502.
[162] R. Maji, J. Contreras-García, N. Capron, E. Degoli, E. Luppi, The role of Si vacancies in the segregation of O, C, and N at silicon grain boundaries: An ab initio study, J. Chem. Phys. 155 (17) (2021) 174704.
[163] G. Zhou, L. Luo, L. Li, J. Ciston, E.A. Stach, J.C. Yang, Step-edge-induced oxide growth during the oxidation of Cu surfaces, Phys. Rev. Lett. 109 (23) (2012) 235502.
[164] G. Zhou, L. Luo, L. Li, J. Ciston, E.A. Stach, W.A. Saidi, J.C. Yang, In situ atomic-scale visualization of oxide islanding during oxidation of Cu surfaces, Chem. Commun. 49 (92) (2013) 10862–10864.
[165] M.T. Curnan, C.M. Andolina, M. Li, Q. Zhu, H. Chi, W.A. Saidi, J.C. Yang, Connecting oxide nucleation and growth to oxygen diffusion energetics on stepped Cu (011) surfaces: An experimental and theoretical study, J. Phys. Chem. C 123 (1) (2018) 452–463.
[166] M. Li, M.T. Curnan, H. Chi, X. Li, G. Henkelman, W.A. Saidi, J.C. Yang, Probing Dynamic Processes of the Initial Stages of Cu (100) Surface Oxidation by in situ Environmental TEM and Multiscale Simulations, Microscopy and Microanalysis 24 (S1) (2018) 262–263.
[167] M. Li, M.T. Curnan, W.A. Saidi, J.C. Yang, Uneven Oxidation and Surface Reconstructions on Stepped Cu (100) and Cu (110), Nano Lett (2022).
[168] C. Choi, S. Kwon, T. Cheng, M. Xu, P. Tieu, C. Lee, J. Cai, H.M. Lee, X. Pan, X. Duan, Highly active and stable stepped Cu surface for enhanced electrochemical CO2 reduction to C2H4, Nature Catal. 3 (10) (2020) 804–812.
[169] F. Guo, Y.-S. Wen, S.-Q. Feng, X.-D. Li, H.-S. Li, S.-X. Cui, Z.-R. Zhang, H.-Q. Hu, G.-Q. Zhang, X.-L. Cheng, Intelligent-ReaxFF: Evaluating the reactive force field parameters with machine learning, Comput. Mater. Sci. 172 (2020) 109393.
[170] D.E. Yilmaz, W.H. Woodward, A.C. Van Duin, Machine Learning-Assisted Hybrid ReaxFF Simulations, J. Chem. Theory Comput. 17 (11) (2021) 6705–6712.
[171] P. Yoo, M. Sakano, S. Desai, M.M. Islam, P. Liao, A. Strachan, Neural network reactive force field for C, H, N, and O systems, npj Comput, Mater. 7 (1) (2021) 1–10.
[172] A. Mishra, S. Hong, P. Rajak, C. Sheng, K.-I. Nomura, R.K. Kalia, A. Nakano, P. Vashishta, Multiobjective genetic training and uncertainty quantification of reactive force fields, npj Comput, Mater. 4 (1) (2018) 1–7.
[173] A. Ermoline, E.L. Dreizin, Equations for the Cabrera-Mott kinetics of oxidation for spherical nanoparticles, Chem. Phys. Lett. 505 (1) (2011) 47–50.
[174] A. Smigelskas, Zinc diffusion in alpha brass, Trans. Aime 171 (1947) 130–142.
[175] Y. Yin, R.M. Rioux, C.K. Erdonmez, S. Hughes, G.A. Somorjai, A.P. Alivisatos, Formation of hollow nanocrystals through the nanoscale Kirkendall effect, Science 304 (5671) (2004) 711–714.
[176] J. Wang, Y. Cui, D. Wang, Design of hollow nanostructures for energy storage, conversion and production, Adv. Mater. 31 (38) (2019) 1801993.
[177] M. Xiao, Z. Wang, M. Lyu, B. Luo, S. Wang, G. Liu, H.M. Cheng, L. Wang, Hollow nanostructures for photocatalysis: advantages and challenges, Adv. Mater. 31 (38) (2019) 1801369.
[178] D. Mordehai, M. Kazakevich, D.J. Srolovitz, E. Rabkin, Nanoindentation size effect in single-crystal nanoparticles and thin films: A comparative experimental and simulation study, Acta Mater. 59 (6) (2011) 2309–2321.
[179] A. Pratt, L. Lari, O. Hovorka, A. Shah, C. Woffinden, S.P. Tear, C. Binns, R. Kröger, Enhanced oxidation of nanoparticles through strain-mediated ionic transport, Nat. Mater. 13 (1) (2014) 26.
[180] L. Han, Q. Meng, D. Wang, Y. Zhu, J. Wang, X. Du, E.A. Stach, H.L. Xin, Interrogation of bimetallic particle oxidation in three dimensions at the nanoscale, Nature Commun. 7 (1) (2016) 13335.
[181] R.K. Kalia, T.J. Campbell, A. Chatterjee, A. Nakano, P. Vashishta, S. Ogata, Multiresolution algorithms for massively parallel molecular dynamics simulations of nanostructured materials, Comput. Phys. Commun. 128 (1–2) (2000) 245–259.
[182] W. Wang, R. Clark, A. Nakano, R.K. Kalia, P. Vashishta, Effects of oxide-shell structures on the dynamics of oxidation of Al nanoparticles, Appl. Phys. Lett. 96 (18) (2010) 181906.
[183] A.P. LaGrow, M.R. Ward, D.C. Lloyd, P.L. Gai, E.D. Boyes, Visualizing the Cu/Cu2O Interface Transition in Nanoparticles with Environmental Scanning Transmission Electron Microscopy, J. Am. Chem. Soc. 139 (1) (2017) 179–185.
[184] L. Gai, Y.K. Shin, M. Raju, A.C.T. van Duin, S. Raman, Atomistic Adsorption of Oxygen and Hydrogen on Platinum Catalysts by Hybrid Grand Canonical Monte Carlo/Reactive Molecular Dynamics, J. Phys. Chem. C 120 (18) (2016) 9780–9793.
[185] L. Liu, A. Corma, Metal Catalysts for Heterogeneous Catalysis: From Single Atoms to Nanoclusters and Nanoparticles, Chem. Rev. 118 (10) (2018) 4981–5079.
[186] J. Behler, B. Delley, S. Lorenz, K. Reuter, M. Scheffler, Dissociation of O 2 at Al (111): The role of spin selection rules, Phys. Rev. Lett. 94 (3) (2005) 036104.
[187] X. Liu, X. Wen, R. Hoffmann, Surface Activation of Transition Metal Nanoparticles for Heterogeneous Catalysis: What We Can Learn from Molecular Dynamics, ACS Catal. 8 (4) (2018) 3365–3375.
[188] K. Dongjin, C. Myungwoo, C. Jerome, K. Sungwon, Y. Kyuseok, K. Jinback, C. Wonsuk, C.M. J., M. Evan, H. Ross, Active site localization of methane oxidation on Pt nanocrystals, Nature Commun. 9(1) (2018) 3422-.
[189] G. Li, L. Niu, Y. Liu, C. Zhang, Atomic-scale identification of microexplosion of aluminum nanoparticles as highly efficient oxidation, Energ. Mater. Front. 2 (1) (2021) 40–50.
[190] L. Song, F.-Q. Zhao, S.-Y. Xu, X.-H. Ju, Atomic origin of the morphological evolution of aluminum hydride (AlH3) nanoparticles during oxidation using reactive force field simulations, Appl. Surf. Sci. 519 (2020) 146249.
[191] Q. Chu, B. Shi, L. Liao, X. Zou, K.H. Luo, N. Wang, Reaction mechanism of the aluminum nanoparticle: physicochemical reaction and heat/mass transfer, J. Phys. Chem. C 124 (6) (2020) 3886–3894.
[192] L. Song, S.-Y. Xu, F.-Q. Zhao, X.-H. Ju, Atomistic insight into shell–core evolution of aluminum nanoparticles in reaction with gaseous oxides at high temperature, J. Mater. Sci. 55 (30) (2020) 14858–14872.
[193] G. Li, L. Niu, X. Xue, W. Hao, Y. Liu, C. Zhang, Atomic Perspective about the Reaction Mechanism and H2 Production during the Combustion of Al Nanoparticles/H2O2 Bipropellants, J. Phys. Chem. A 124 (37) (2020) 7399–7410.
[194] L. Song, F.-Q. Zhao, S.-Y. Xu, C.-C. Ye, X.-H. Ju, Structural evolution of aluminum hydride nanoparticles in water using ReaxFF molecular dynamics method, Mater. Today Commun. 26 (2021) 101804.
[195] B. Wu, F. Wu, P. Wang, A. He, H. Wu, Ignition and Combustion of Hydrocarbon Fuels Enhanced by Aluminum Nanoparticle Additives: Insights from Reactive Molecular Dynamics Simulations, J. Phys. Chem. C 125 (21) (2021) 11359–11368.
[196] L. Song, S.-Y. Xu, F.-Q. Zhao, X.-H. Ju, Atomistic insight into dehydrogenation and oxidation of aluminum hydride nanoparticles (AHNPs) in reaction with gaseous oxides at high temperature, Int. J. Hydrogen Energy 46 (11) (2021) 8091–8103.
[197] L. Song, Z. Mei, S.Y. Xu, F.Q. Zhao, X.H. Ju, Toward homogenous AlN via reaction of Al nanoparticles with N2 and NH3: Reactive molecular dynamics simulation, J. Am. Ceram. Soc. 105 (2) (2022) 1343–1357.
[198] G. Li, L. Niu, W. Hao, Y. Liu, C. Zhang, Atomistic insight into the microexplosion-accelerated oxidation process of molten aluminum nanoparticles, Combust. Flame 214 (2020) 238–250.
[199] L. Song, F.-Q. Zhao, S.-Y. Xu, X.-H. Ju, Encapsulating aluminum nanoparticles into carbon nanotubes for combustion: a molecular dynamics study, Phys. Chem. Chem. Phys. 23 (20) (2021) 11886–11892.
[200] R. Chen, X. Cheng, C. Zhang, H. Wu, H. Zhu, S. He, Sub-3 nm Aluminum Nanocrystals Exhibiting Cluster-Like Optical Properties, Small 17 (27) (2021) 2002524.
[201] J.T. Zhang, J.F. Liu, Q. Peng, X. Wang, Y.D. Li, Nearly monodisperse Cu2O and CuO nanospheres: Preparation and applications for sensitive gas sensors, Chem. Mater. 18 (4) (2006) 867–871.
[202] A.P. Ingle, N. Duran, M. Rai, Bioactivity, mechanism of action, and cytotoxicity of copper-based nanoparticles: a review, Appl. Microbiol. Biotechnol. 98 (3) (2014) 1001–1009.
[203] M.B. Gawande, A. Goswami, F.X. Felpin, T. Asefa, X. Huang, R. Silva, X. Zou, R. Zboril, R.S. Varma, Cu and Cu-Based Nanoparticles: Synthesis and Applications in Catalysis, Chem. Rev. 116 (6) (2016) 3722–3811.
[204] H. Ohnishi, Y. Kondo, K. Takayanagi, Quantized conductance through individual rows of suspended gold atoms, Nature 395 (6704) (1998) 780–783.
[205] H. Li, K.M. Liew, X.Q. Zhang, J.X. Zhang, X.F. Liu, X.F. Bian, Electron-Conduction Properties of Fe−Al Alloy Nanowires, J. Phys. Chem. B 112 (49) (2008) 15588–15595.
[206] M. Li, Z. Zhao, T. Cheng, A. Fortunelli, C.-Y. Chen, R. Yu, Q. Zhang, L. Gu, B.V. Merinov, Z. Lin, Ultrafine jagged platinum nanowires enable ultrahigh mass activity for the oxygen reduction reaction, Science 354 (6318) (2016) 1414–1419.
[207] L. Zhang, X. Dai, Y. Zhou, Z. Zhao, L. Yin, H. Li, Theoretical study of electronic transport properties of lead nanowires doped with silicon, Comput. Mater. Sci. 136 (2017) 198–206.
[208] G. Shen, P.-C. Chen, K. Ryu, C. Zhou, Devices and chemical sensing applications of metal oxide nanowires, J. Mater. Chem. 19 (7) (2009) 828–839.
[209] H. Li, X.Q. Zhang, F.W. Sun, Y.F. Li, K.M. Liew, X.Q. He, Theoretical study of the electrical transport of nickel nanowires and a single atomic chain, J. Appl. Phys. 102 (1) (2007) 013702.
[210] H. Li, F. Sun, Y. Li, X. Liu, K.M. Liew, Theoretical studies of the stretching behavior of carbon nanowires and their superplasticity, Scr. Mater. 59 (5) (2008) 479–482.
[211] J.H. Luo, F.F. Wu, J.Y. Huang, J.Q. Wang, S.X. Mao, Superelongation and Atomic Chain Formation in Nanosized Metallic Glass, Phys. Rev. Lett. 104 (21) (2010) 215503.
[212] J. Ustarroz, I.M. Ornelas, G. Zhang, D. Perry, M. Kang, C.L. Bentley, M. Walker, P.R. Unwin, Mobility and Poisoning of Mass-Selected Platinum Nanoclusters during the Oxygen Reduction Reaction, ACS Catal. 8 (8) (2018) 6775–6790.
[213] B.A. Rohr, A.R. Singh, J.K. Nørskov, A theoretical explanation of the effect of oxygen poisoning on industrial Haber-Bosch catalysts, J. Catal. 372 (2019) 33–38.
[214] V.P. Zhdanov, B. Kasemo, Cabrera-Mott kinetics of oxidation of metal nanowires, Appl. Phys. Lett. 100 (24) (2012) 243105.
[215] H.S. Park, W. Cai, H.D. Espinosa, H. Huang, Mechanics of Crystalline Nanowires, MRS Bull. 34 (3) (2009) 178–183.
[216] U. Khalilov, G. Pourtois, A.v. Duin, E. Neyts, Self-limiting oxidation in small-diameter Si nanowires, Chem. Mater. 24(11) (2012) 2141-2147.
[217] F.G. Sen, Y. Qi, A.C. van Duin, A.T. Alpas, Oxidation induced softening in Al nanowires, Appl. Phys. Lett. 102 (5) (2013) 051912.
[218] F.G. Sen, A.T. Alpas, A.C. Van Duin, Y. Qi, Oxidation-assisted ductility of aluminium nanowires, Nature Commun. 5 (2014) 3959.

[219] G. Aral, Y.-J. Wang, S. Ogata, A.C. Van Duin, Effects of oxidation on tensile deformation of iron nanowires: Insights from reactive molecular dynamics simulations, J. Appl. Phys. 120 (13) (2016) 135104.
[220] G. Aral, M.M. Islam, Y.-J. Wang, S. Ogata, A.C. van Duin, Oxyhydroxide of metallic nanowires in a molecular H 2 O and H 2 O 2 environment and their effects on mechanical properties, Phys. Chem. Chem. Phys. 20 (25) (2018) 17289–17303.
[221] G. Aral, M.M. Islam, A.C. Van Duin, Role of surface oxidation on the size dependent mechanical properties of nickel nanowires: a ReaxFF molecular dynamics study, Phys. Chem. Chem. Phys. 20 (1) (2018) 284–298.
[222] G. Aral, M.M. Islam, Y.-J. Wang, S. Ogata, A.C.T. van Duin, Atomistic insights on the influence of pre-oxide shell layer and size on the compressive mechanical properties of nickel nanowires, J. Appl. Phys. 125 (16) (2019) 165102.
[223] Y. Yang, A. Kushima, W. Han, H. Xin, J. Li, Liquid-Like, Self-Healing Aluminum Oxide during Deformation at Room Temperature, Nano Lett. 18 (4) (2018) 2492–2497.
[224] A.E. Hughes, I.S. Cole, T.H. Muster, R.J. Varley, Designing green, self-healing coatings for metal protection, NPG Asia Mater. 2 (4) (2010) 143–151.
[225] M.D. Hager, Self-healing materials, Handbook of Solid State, Chemistry (2017) 201–225.
[226] G. Fiori, F. Bonaccorso, G. Iannaccone, T. Palacios, D. Neumaier, A. Seabaugh, S. K. Banerjee, L. Colombo, Electronics based on two-dimensional materials, Nat. Nanotechnol. 9 (10) (2014) 768.
[227] F. Koppens, T. Mueller, P. Avouris, A. Ferrari, M. Vitiello, M. Polini, Photodetectors based on graphene, other two-dimensional materials and hybrid systems, Nat. Nanotechnol. 9 (10) (2014) 780.
[228] J. Du, H. Yu, B. Liu, M. Hong, Q. Liao, Z. Zhang, Y. Zhang, Strain engineering in 2D material-based flexible optoelectronics, Small Methods 5 (1) (2021) 2000919.
[229] P. Kumbhakar, C.C. Gowda, P.L. Mahapatra, M. Mukherjee, K.D. Malviya, M. Chaker, A. Chandra, B. Lahiri, P. Ajayan, D. Jariwala, Emerging 2D metal oxides and their applications, Mater. Today 45 (2021) 142–168.
[230] V. Chabot, D. Higgins, A. Yu, X. Xiao, Z. Chen, J. Zhang, A review of graphene and graphene oxide sponge: material synthesis and applications to energy and the environment, Energy Environ. Sci. 7 (5) (2014) 1564–1596.
[231] J.M. Park, Y. Cao, K. Watanabe, T. Taniguchi, P. Jarillo-Herrero, Tunable strongly coupled superconductivity in magic-angle twisted trilayer graphene, Nature 590 (7845) (2021) 249–255.
[232] A. Kara, H. Enriquez, A.P. Seitsonen, L.L.Y. Voon, S. Vizzini, B. Aufray, H. Oughaddou, A review on silicene—new candidate for electronics, Surf. Sci. Rep. 67 (1) (2012) 1–18.
[233] X.-F. Jiang, Q. Weng, X.-B. Wang, X. Li, J. Zhang, D. Golberg, Y. Bando, Recent progress on fabrications and applications of boron nitride nanomaterials: a review, J. Mater. Sci. Technol. 31 (6) (2015) 589–598.
[234] M. Naguib, M. Kurtoglu, V. Presser, J. Lu, J. Niu, M. Heon, L. Hultman, Y. Gogotsi, M.W. Barsoum, Two-dimensional nanocrystals produced by exfoliation of Ti3AlC2, Adv. Mater. 23 (37) (2011) 4248–4253.
[235] M. Naguib, V.N. Mochalin, M.W. Barsoum, Y. Gogotsi, 25th anniversary article: MXenes: a new family of two-dimensional materials, Adv. Mater. 26 (7) (2014) 992–1005.
[236] F. Cao, Y. Zhang, H. Wang, K. Khan, A.K. Tareen, W. Qian, H. Zhang, H. Ågren, Recent Advances in Oxidation Stable Chemistry of Two-Dimensional MXenes, Adv. Mater. 2107554 (2021).
[237] J.C. Meyer, C. Kisielowski, R. Erni, M.D. Rossell, M. Crommie, A. Zettl, Direct imaging of lattice atoms and topological defects in graphene membranes, Nano Lett. 8 (11) (2008) 3582–3586.
[238] F. Banhart, J. Kotakoski, A.V. Krasheninnikov, Structural defects in graphene, ACS Nano 5 (1) (2010) 26–41.
[239] P.Y. Huang, C.S. Ruiz-Vargas, A.M. Van Der Zande, W.S. Whitney, M.P. Levendorf, J.W. Kevek, S. Garg, J.S. Alden, C.J. Hustedt, Y. Zhu, Grains and grain boundaries in single-layer graphene atomic patchwork quilts, Nature 469 (7330) (2011) 389.
[240] A. Romanov, M. Rozhkov, A. Kolesnikova, Disclinations in polycrystalline graphene and pseudo-graphenes. Review, J. Mater. Sci. Lett. 8 (4) (2018) 384–400.
[241] M. Terrones, A.R. Botello-Méndez, J. Campos-Delgado, F. Lopez-Urias, Y.I. Vega-Cantú, F.J. Rodríguez-Macías, A.L. Elías, E. Munoz-Sandoval, A.G. Cano-Márquez, J.-C. Charlier, Graphene and graphite nanoribbons: Morphology, properties, synthesis, defects and applications, Nano Today 5 (4) (2010) 351–372.
[242] P. Zheng, X. Zhang, Y. Duan, M. Yan, R. Chapman, Y. Jiang, H. Li, Oxidation of graphene with variable defects: alternately symmetrical escape and self-restructuring of carbon rings, Nanoscale 12 (18) (2020) 10140–10148.
[243] J.J. Palacios, J. Fernández-Rossier, L. Brey, Vacancy-induced magnetism in graphene and graphene ribbons, Phys. Rev. B 77 (19) (2008) 195428.
[244] X. Zhang, Z. Xu, Q. Yuan, J. Xin, F. Ding, The favourable large misorientation angle grain boundaries in graphene, Nanoscale 7 (47) (2015) 20082–20088.
[245] J.P. Froning, P. Lazar, M. Pykal, Q. Li, M. Dong, R. Zbořil, M. Otyepka, Direct mapping of chemical oxidation of individual graphene sheets through dynamic force measurements at the nanoscale, Nanoscale 9 (1) (2017) 119–127.
[246] R. Rao, A.E. Islam, P.M. Campbell, E.M. Vogel, B. Maruyama, In situ thermal oxidation kinetics in few layer MoS2, 2D Mater. 4 (2) (2017) 025058.
[247] T. Li, Y. Yao, Z. Huang, P. Xie, Z. Liu, M. Yang, J. Gao, K. Zeng, A.H. Brozena, G. Pastel, Denary oxide nanoparticles as highly stable catalysts for methane combustion, Nature Catal. 4 (1) (2021) 62–70.
[248] G.-J. Kroes, Frontiers in surface scattering simulations, Science 321 (5890) (2008) 794–797.
[249] F. Libisch, C. Huang, P. Liao, M. Pavone, E.A. Carter, Origin of the energy barrier to chemical reactions of O 2 on Al (111): Evidence for charge transfer, not spin selection, Phys. Rev. Lett. 109 (19) (2012) 198303.
[250] M. Kurahashi, Y. Yamauchi, Steric Effect in O_2 Sticking on Al (111): Preference for Parallel Geometry, Phys. Rev. Lett. 110 (24) (2013) 246102.
[251] P.G. Lustemberg, P.N. Plessow, Y. Wang, C. Yang, A. Nefedov, F. Studt, C. Wöll, M.V. Ganduglia-Pirovano, Vibrational frequencies of cerium-oxide-bound CO: A challenge for conventional DFT methods, Phys. Rev. Lett. 125 (25) (2020) 256101.
[252] J. Sauer, Ab Initio Calculations for Molecule-Surface Interactions with Chemical Accuracy, Acc. Chem. Res. 52 (12) (2019) 3502–3510.
[253] C.R.A. Catlow, J. Buckeridge, M.R. Farrow, A.J. Logsdail, A.A. Sokol, Quantum Mechanical/Molecular Mechanical (QM/MM) Approaches, Handbook Solid State Chem. (2017) 647–680.
[254] J. Buckeridge, C.R.A. Catlow, M. Farrow, A.J. Logsdail, D. Scanlon, T. Keal, P. Sherwood, S. Woodley, A. Sokol, A. Walsh, Deep vs shallow nature of oxygen vacancies and consequent n-type carrier concentrations in transparent conducting oxides, Phys. Rev. Mater. 2 (5) (2018) 054604.
[255] Y. Lu, M.R. Farrow, P. Fayon, A.J. Logsdail, A.A. Sokol, C.R.A. Catlow, P. Sherwood, T.W. Keal, Open-source, python-based redevelopment of the chemshell multiscale QM/MM environment, J. Chem. Theory Comput. 15 (2) (2018) 1317–1328.
[256] Q. Hou, J. Buckeridge, A. Walsh, Z. Xie, Y. Lu, T.W. Keal, J. Guan, S.M. Woodley, C.R.A. Catlow, A.A. Sokol, The Interplay of Interstitial and Substitutional Copper in Zinc Oxide, Front. Chem. (2021) 1102.
[257] P. Clabaut, B. Schweitzer, A.W. Gotz, C. Michel, S.N. Steinmann, Solvation free energies and adsorption energies at the metal/water interface from hybrid quantum-mechanical/molecular mechanics simulations, J. Chem. Theory Comput. 16 (10) (2020) 6539–6549.
[258] B.T. Lau, G. Knizia, T.C. Berkelbach, Regional embedding enables high-level quantum chemistry for surface science, J. Phys. Chem. Lett. 12 (3) (2021) 1104–1109.
[259] S.A. Nastase, A.J. Logsdail, C.R.A. Catlow, QM/MM study of the reactivity of zeolite bound methoxy and carbene groups, Phys. Chem. Chem. Phys. 23 (32) (2021) 17634–17644.
[260] C.I. Ossai, A data-driven machine learning approach for corrosion risk assessment—a comparative study, Big Data Cogn. Comput. 3 (2) (2019) 28.
[261] T. Würger, C. Feiler, F. Musil, G.B. Feldbauer, D. Höche, S.V. Lamaka, M.L. Zheludkevich, R.H. Meißner, Data science based Mg corrosion engineering, Front. Mater. 6 (2019) 53.
[262] C.D. Taylor, B.M. Tossey, High temperature oxidation of corrosion resistant alloys from machine learning, npj Mater, Degrad. 5 (1) (2021) 1–10.
[263] L.B. Coelho, D. Zhang, Y. Van Ingelgem, D. Steckelmacher, A. Nowé, H. Terryn, Reviewing machine learning of corrosion prediction in a data-oriented perspective, npj Mater, Degrad. 6 (1) (2022) 1–16.